arXiv:1512.06565v1 [quant-ph] 21 Dec 2015

Loops and strings in a superconducting lattice gauge simulator

G.K. Brennen,[1] G. Pupillo,[2] E. Rico,[3,4] T.M. Stace,[5] and D. Vodola[2]

[1]*Centre for Engineered Quantum Systems, Macquarie University, Sydney, NSW 2109, Australia*
[2]*icFRC, IPCMS (UMR 7504) and ISIS (UMR 7006), Universite de Strasbourg and CNRS, Strasbourg, France*
[3]*Department of Physical Chemistry, University of the Basque Country UPV/EHU, Apartado 644, E-48080 Bilbao, Spain*
[4]*IKERBASQUE, Basque Foundation for Science, Maria Diaz de Haro 3, E-48013 Bilbao, Spain*
[5]*Center for Engineered Quantum Systems, School of Mathematics and Physics, The University of Queensland, St Lucia, Queensland 4072, Australia*

We propose a quantum simulation of electromagnetism in $2+1$ dimensions using an array of superconducting fluxonium devices. The encoding is in the integer ($S=1$) representation of the quantum link model formulation of compact $U(1)$ lattice gauge theory. We show how to engineer the Gauss constraint via an ancilla mediated gadget construction and how to tune between the strongly coupled and intermediately coupled regimes. The witnesses to the existence of the predicted confining phase of the model are provided by non-local order parameters from Wilson loops and disorder parameters from 't Hooft strings and we show how to measure these operators non-destructively via dispersive coupling of the fluxonium islands to a microwave cavity mode. Evidence for existence of the confined phase in the ground state of the simulation Hamiltonian is found by DMRG calculations on a ladder geometry.

PACS numbers: 03.67.Lx, 37.10.Ty, 71.38.Ht

Gauge theories play a fundamental role in modern physics, with examples ranging from quantum electrodynamics to the standard model of elementary particle physics. From the breakthrough contribution by Wilson in 1974 [1], lattice gauge theories (LGT) [2, 3] represent a cornerstone in our understanding of the physical world and lie at the heart of theories dealing with such diverse systems as quantum spin liquids and the quark-gluon plasma. Furthermore, there is good reason to believe that certain types of gauge structures could open up new possibilities for quantum computation.

In gauge field theories, phases cannot be characterized by local order parameters, as the mean value of non gauge invariant quantities vanishes for a compact gauge group. Alternative observables are thus needed to describe them. In this respect, a key feature of gauge models is the property of confinement, meaning there are no isolated particles with non-vanishing color charge in nature. Non-local order parameters such as Wilson loops [1] and 't Hooft strings [4] have been introduced to capture the appearance or the absence of confinement in the phase diagram of gauge models.

Classical simulations of dynamical gauge fields, in particular of real time dynamics, is a hard computational problem [5]. Recently, it has been shown that quantum simulators of dynamical gauge fields make accessible to quantum technologies the corresponding real-time dynamics in atomic physics setups[6–20] and superconducting circuit platforms [21–24] (see also recent reviews [25, 26]). In this work we show how to simulate the quantum dynamics [27] of a pure compact $U(1)$ LGT in $2+1$ dimensions with an architecture based on superconducting circuits with fluxonium devices. We also show how to perform non-demolition measurement of space-like Wilson loops and 't Hooft strings on these architectures, which has hitherto been difficult in other simulation protocols.

Polyakov [28] showed that if Lorentz invariance is respected, $U(1)$ gauge theories in $2+1$ dimensions are always in a confinement phase at $T=0$ but there can be a phase transition at $T_c \neq 0$. This is a scenario that could be quantum simulated by our proposed quantum simulator. Moreover, we will consider quantum link model (QLM) formulation of LGT [29–31] wherein a cutoff in the maximum magnitudes of irreps of the group is enforced. This allows for a quantum simulation using a finite local Hilbert space dimension and is a general case of typical models that appear in condensed matter physics like quantum spin ice models or quantum dimer models. In these instances, Lorentz symmetry is not present and it is well known the existence of de-confined critical points even at $T=0$, they are usually called Rokhsar-Kivelson points [32]. In our proposed architecture, these systems have many "internal levels" with which to represent electric flux and allow us in principle to reach the continuum limit of the theory.

In the pure gauge $U(1)$ QLM the degrees of freedom are electric fluxes $\hat{E}_{\alpha,\beta}$ that live on the links $\langle\alpha,\beta\rangle$ of a square lattice with local link state space $\mathbb{C}^{N+1}$. The states of the complete Hilbert space are labelled by the electric fluxes on the links, i.e., $\hat{E}_{\alpha,\beta}|E_{\alpha,\beta}\rangle = E_{\alpha,\beta}|E_{\alpha,\beta}\rangle$. For a compact $U(1)$ gauge group, the fluxes take integer or half integer values: $-\frac{N}{2} \leq E_{\alpha,\beta} \leq \frac{N}{2}$ for N even or odd. Integer representations allow to have an electric field term which more closely mimics the continuous theory for the U(1) pure gauge model while half-integer representations can be understood as gauge fields within a classical background. The operator that changes the phase of the local link operators $\hat{U}_{\alpha,\beta}$ is given by $e^{i\theta_\alpha \hat{E}_{\alpha,\beta}}$ satisfying the commutation relations $\left[\hat{E}_{\alpha,\beta},\hat{U}_{\alpha,\beta}\right] = -\hat{U}_{\alpha,\beta}$. The representation of the electric and magnetic operators and in the $U(1)$ QLM with local dimension $N+1$, and their large$-N$ limit, is given in Sec. I of [33]. In $U(1)$ gauge theory the net electric flux at a given vertex is zero, hence there is a conserved quantity $\hat{G}_\alpha = \hat{E}_{\mu,\alpha} + \hat{E}_{\nu,\alpha} - \hat{E}_{\alpha,\beta} - \hat{E}_{\alpha,\gamma}$. The phase of the operators can be changed locally with the $U(1)$ gauge transformation $\exp\left[i\theta_\alpha \hat{G}_\alpha\right]$ and the dynamics remain invariant. The gauge invariant subspace is defined as: $\hat{G}_\alpha|\text{phys}\rangle = 0$, which is nothing but the discretized version of Gauss' law. In a pure gauge model, there are two competing terms in the

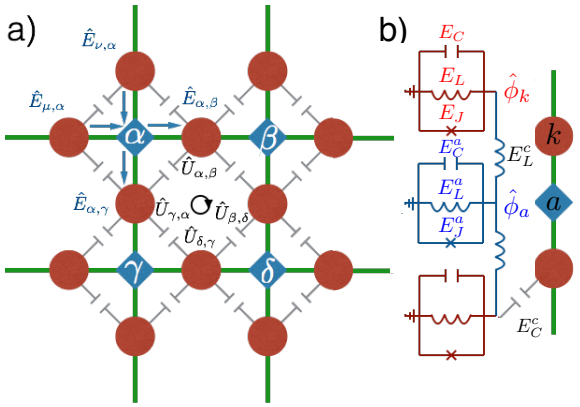

FIG. 1. $U(1)$ quantum link model engineered in a fluxonium array. a): "Electric", $\hat{E}_{\alpha,\beta}$, and "magnetic", $\hat{U}_{\alpha,\beta}$, degrees of freedom are associated with links $\langle\alpha,\beta\rangle$ of a square lattice. Here the link degrees of freedom (red circles) are encoded into local phase eigenfunctions of the fluxonia. The ancilla (blue diamonds) on vertices are inductively coupled to neighboring link islands to mediate the Gauss constraint and plaquette interactions are obtained via link nearest neighbor capacitive coupling. b): Schematic superconducting circuit elements used to build and couple components of the simulation. The link (red) devices have local phase $\hat{\phi}_{\text{link}}$ and capacitive, inductive, and flux-biased Josephson energies E_C, E_L and E_J respectively and similarly for the ancilla (blue) devices. The inductive and capacitive coupling energies are E_L^c and E_C^c.

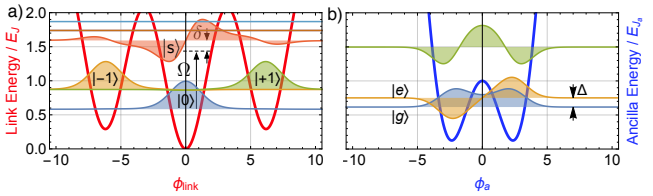

FIG. 2. a): Link fluxonia operate as qutrits with offset phase $\phi_{\text{off}} = 0$. The potential $P(\phi_{\text{link}})$ (red) and the eigenfunctions are plotted for the qutrit states $|0\rangle, |\pm 1\rangle$, which represent electric flux states, and the next energy state $|s\rangle$. A cavity field couples states $|0\rangle \leftrightarrow |s\rangle$ with Rabi frequency Ω and detuning δ which allows to tune the *electric coupling* in the QLM. b): Ancilla fluxonia operate as qubits with $\phi_{\text{off}} = \pi$. Show are the potential $P(\phi_a)$ and qubit eigenfunctions $|g\rangle$ and $|e\rangle$. The qubit energy splitting is Δ. The ancilla are initialized in state $|e\rangle$ and, via virtual transitions to the $|g\rangle$ states, mediate a coupling between the adjacent link qutrits which provides for the *Gauss constraint*. The *magnetic coupling* in the QLM is provided by nearest neighbor capacitive coupling between link fluxonia.

Hamiltonian: the electric term, that penalizes electric flux on every link; and the magnetic term, that penalizes magnetic flux on every plaquette $\square$,

$$\hat{H}_{\text{QLM}} = g^2_{\text{elect}} \sum_{\langle\alpha,\beta\rangle} \hat{E}^2_{\alpha,\beta} - \frac{1}{g^2_{\text{magn}}} \sum_{\square} \left(\hat{U}_{\alpha,\beta}\hat{U}_{\beta,\delta}\hat{U}_{\delta,\gamma}\hat{U}_{\gamma,\alpha} + \text{h.c.}\right) \tag{1}$$

where g^2_{elec} and g^2_{magn} are the coupling constants for the electric term and magnetic term, respectively.

The smallest Wilson loop operator is defined on a plaquette: $\mathcal{W} = \hat{U}_{\alpha,\beta}\hat{U}_{\beta,\delta}\hat{U}_{\delta,\gamma}\hat{U}_{\gamma,\alpha}$. This is a discrete approximation to the integral over the plaquette $e^{i\oint \mathbf{A}\cdot\mathbf{dl}}$ where $\mathbf{A}$ is the magnetic vector potential. In a similar way, it can be defined in bigger loops by a path ordering multiplication of the link operators $\hat{U}_{\alpha,\beta}$ on every link of the loop $\mathcal{C}$. In the confined phase there is an area dependence of the Wilson loop $\mathcal{W}_r(\mathcal{C}) \sim e^{-\text{area}(\mathcal{C})}$ whereas, in the de-confined phase, it is expected a perimeter law, i.e., $\mathcal{W}_r(\mathcal{C}) \sim e^{-\text{perimeter}(\mathcal{C})}$. A 't Hooft disorder operator can be defined as the product of the links in one direction such that $\hat{\Upsilon}(\phi) = \prod_n \exp\left[i\phi\hat{E}_{na_x,na_x+a_y}\right]$. In [33] Sec. I B we show that in the QLM it acts a disorder parameter, which is dual to a local order parameter. Indeed this operator changes the value of the magnetic flux by an amount ϕ just on the plaquette where it starts and ends, i.e., it introduces a magnetic vortex on these two plaquettes. Now in the confining phase it is ordered $\langle\hat{\Upsilon}(\phi)\rangle \neq 0$ for $\phi \neq 0$ in $2+1$ dimensions. The fact that a non-zero expectation value of the disorder parameter characterizes a confinement phase in a gauge model may simplify the signal-to-noise problem in an actual quantum simulation.

Implementation with superconducting devices: To quantum simulate a $U(1)$ QLM within a superconducting setup, we have to consider three main elements: (i) The local Hilbert space, that in our case, is labelled by the electric flux on the link of the lattice gauge model. In our implementation, the Hilbert space is going to be spanned by a discrete but infinite set of states given by the magnetic fluxes on the loops of a fluxonium device; (ii) The Gauss' law, on the vertex of the lattice, is imposed by strong interactions between the fluxonia mediated by tunable inductive couplings; (iii) The gauge invariant dynamics will emerge at second order of perturbation with capacitive couplings between nearest neighbor links.

We propose using fluxonium [34] which is an inductively shunted superconducting Josephson junction island with local Hamiltonian $\hat{H}_k$ and potential $\hat{P}(\hat{\phi}_k)$ at island k:

$$\hat{H}_k = 4E_C\hat{n}_k^2 + \hat{P}(\hat{\phi}_k); \quad \hat{P}(\hat{\phi}_k) = -E_J\cos(\hat{\phi}_k + \phi_{\text{off}}) + \frac{E_L}{2}\hat{\phi}_k^2. \tag{2}$$

Here $E_C = \frac{e^2}{2C}$ is the charging energy associated with the energy to transfer a single election onto the island with C the total capacitance between island electrodes, $E_J = (\frac{\hbar}{2e})^2\frac{1}{L_J}$ is the Josephson energy with L_J the effective inductance of the Josephson junction, and $E_L = (\frac{\hbar}{2e})^2\frac{1}{L}$ is the inductance energy where L is the external shunting inductance. Fluxonium exists in the regime where $E_J \geq E_C > E_L$. The superconducting phase ϕ_k, which is equivalent to the magnetic flux through the island, is a non compact variable in the inductively shunted case and hence the conjugate charge $\hat{n}_k = -i\frac{\partial}{\partial\phi_k}$ takes continuous values. The offset phase $\phi_{\text{off}} = 2\pi\frac{\Phi_{\text{ext}}}{\Phi_0}$ where Φ_{ext} is a tunable external flux [35] and $\Phi_0 = \frac{\hbar}{2e}$ is the magnetic flux quantum. The potential terms can be tuned to support "integer" representations of the electric flux (i.e., with a unique local ground state), in the lowest energy states by choosing $\phi_{\text{off}} = 0$ or "half-integer" representations of the electric flux

(i.e., with two degenerate local ground states) when $\phi_{\rm off} = \pi$.

In the limit $E_J \sim E_C \gg E_L$, the lowest energy states are the first band Wannier functions with a well defined magnetic flux, $\phi_k = 2\pi m_k$, with a standard deviation of the wavefunction $\sigma = (\frac{8E_C}{E_J})^{1/4}$. To enforce the *Gauss law constraint* we introduce an ancillary fluxonium at every vertex of the lattice. Each ancilla has parameters E_J^a, E_C^a, E_L^a and offset flux $\phi_{\rm off}^a = \pi$ with lowest energy states $|g\rangle$ and $|e\rangle$ denoting symmetric and anti-symmetric wave-functions (see Fig. 2b).

The ancilla is inductively coupled to each of its four nearest neighbors located on the links: $\hat{H}_{\rm ind} = \frac{E_L^c}{2}\sum_v \sum_{k=1}^4 \left(\hat{\phi}_k - \hat{\phi}_a\right)^2$ where $\hat{\phi}_k$ is the phase on link k and $\hat{\phi}_a$ is the ancilla phase located at vertex v, and $E_L^c = (\frac{\hbar}{2e})^2 \frac{1}{L_c}$ with L_c the coupling inductance. Consider the case the ancilla is prepared in the excited state $|e\rangle$. This state has been shown to be long lived ($T_1 > 1$ms reported), due to coherent suppression of electromagnetic dissipation by superconducting quasiparticles which is the main source of decay [35]. To first order the interaction $\hat{H}_{\rm ind}$ is zero since $|e\rangle$ is antisymmetric in ϕ_a. To second order in the ratio E_L^c/Δ we obtain an effective Hamiltonian acting on the links surrounding each vertex. We only include the terms diagonal in the $|m_k\rangle$ basis since the off diagonal terms are much smaller by a factor $\sim e^{-\pi^2/\sigma^2}$. The total local plus inductive interaction is then (see Sec. II B of [33] for details): $\sum_k \hat{H}_k + \hat{H}_{\rm ind} = V\sum_k S_k^{z\,2} + U\sum_v (\sum_{k\in\mathcal{N}(v)} \hat{S}_k^z)^2$, where $U = E_L^{c\,2} |\langle g|\hat{\phi}_a|e\rangle|^2 |\langle\hat{\phi}\rangle_{m=1}|^2/\Delta > 0$ and $\mathcal{N}(v)$ is the neighborhood of a vertex v on the lattice. $\Delta = E_e - E_g > 0$ is the ancilla qubit energy splitting including local contributions from the inductive coupling, calculated using Eq. 2, with the replacement $E_L^a \to E_L^a + 4E_L^c$, and V, which represents the *electric coupling*, is the qutrit energy splitting $E_1 - E_0$ also computed using Eq. 2 with the replacements: $E_L \to E_L + 2E_L^c$.

In order to obtain the *magnetic coupling* we introduce a capacitive coupling between the fluxonia on the links of the form: $\hat{H}_{\rm cap} = 8E_C^c \sum_{\langle k,j\rangle} \hat{n}_k \hat{n}_j$. Because the operators $\hat{n}$ generate displacements in phase, this interaction allows for electric flux values m_k to fluctuate. Here $E_C^c/E_C \simeq \frac{\sqrt{8+\xi^{-2}}K_0(\xi^{-1})}{4\xi K(-16\xi^2/(8+\xi^{-2}))}$ where $\xi \equiv \sqrt{C_c/C}$ and C_c is the capacitance between nearest neighbors, $K_0(x)$ is the modified zeroth Bessel function of the second kind, and $K(x)$ is the elliptic integral of the first kind (see Sec. II C of [33]). There are longer range couplings as well but they fall off exponentially with island separation with a correlation length ξ. The total two body implementation Hamiltonian is then

$$\hat{H}_{\rm imp} = V\sum_k S_k^{z\,2} + U\sum_v \Big(\sum_{k\in\mathcal{N}(v)} \hat{S}_k^z\Big)^2 + J\sum_{\langle j,k\rangle} (\hat{S}_j^+ \hat{S}_k^- + \hat{S}_j^- \hat{S}_k^+), \tag{3}$$

with $J = -8E_C^c |\langle 1|\hat{n}|0\rangle|^2$. In the limit $U \gg |J|$, the second term projects the ground states into the gauge invariant subspace and the effective Hamiltonian is

$$\begin{aligned}\hat{H}_{\rm eff} = &-\frac{2J^2}{U}\sum_{\square}(\hat{S}^+\hat{S}^-\hat{S}^+\hat{S}^- + h.c.) \\ &+ \left(V + 2\frac{J^2}{U}\right)\sum_j \hat{S}_j^{z\,2} + \frac{J^2}{4U}\sum_{\langle j,k\rangle} \hat{S}_j^z \hat{S}_k^z \left(1 - \hat{S}_j^z \hat{S}_k^z\right),\end{aligned} \tag{4}$$

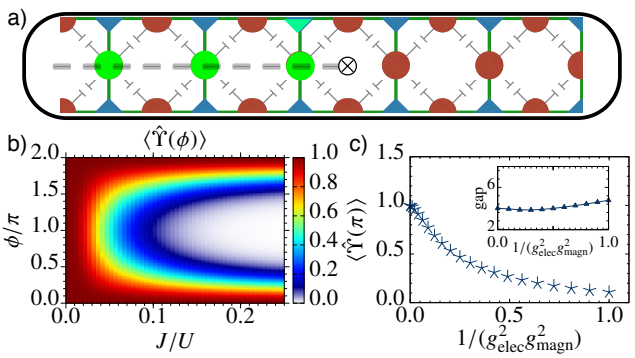

FIG. 3. Ground state properties of the spin-1 lattice model on a ladder with open boundaries. a): Schematic of a fluxonium array embedded in a microwave cavity. Fluxonia in green interact dispersively with a cavity mode enabling measurement of the 't Hooft string operator on the link fluxonia (green circles) by measurement on one ancilla (green triangle). b): Expectation value of the 't Hooft string $\hat{\Upsilon}(\phi) = \prod_{n=1}^{L/2} \exp\left[i(-1)^n \phi \hat{S}^z_{n\mu_x, n\mu_x+\mu_y}\right]$ which inserts a flux ϕ at the plaquette in the middle of the L rung ladder (here $L = 29$ with 85 spins total). The contour plot is for the ground state of the two body Hamiltonian $\hat{H}_{\rm imp}$ with $V = 0$. Here $\langle\hat{\Upsilon}\rangle \neq 0$ is indicative of a confining phase. c): Plot of a cross section of b) but in the pure gauge model $\hat{H}_{\rm QLM}$. Inset: Plot of the energy gap in units $g_{\rm elec}^2$ for the pure gauge model in the thermodynamic limit. Numerics were performed using DMRG with 300 states and truncation error is estimated as $< 10^{-12}$.

like the pure gauge Hamiltonian $\hat{H}_{\rm QLM}$, Eq. (1), up to a redefinition of the electric field term and two body term $\hat{S}^z\hat{S}^z$ that could renormalize the strong initial U term in the microscopic Hamiltonian. In any case, these terms respect all the symmetries of the gauge invariant model and the effective model is a $2+1$ $U(1)$ quantum link model with $g_{\rm elec}^2 = V + 2J^2/U$ and $1/g_{\rm magn}^2 = 2J^2/U$. Numerical simulations using DMRG of the ground state of the Hamiltonian $\hat{H}_{\rm imp}$, are performed on a ladder which is the minimal geometry displaying features of a 2+1 dimensional system (see Fig. 3b). For $J/U \ll 1$, the value of the 't Hooft string is indicative of a confining phase while otherwise it is deconfined. The qualitative behavior is the same using the pure gauge $\hat{H}_{\rm QLM}$ model (see Sec. [33]).

We now show to simulate the two body Hamiltonian $\hat{H}_{\rm imp}$ for a three level (spin-1) $U(1)$ QLM as shown in Fig. 2. The interaction energies can be determined by numerically diagonalizing the local Hamiltonians (See Sec. II D of [33]), and then computing the relevant wave-function overlaps to evaluate the interaction terms. We first show how to prepare the system in the strong coupling limit, which is close to the product state $\otimes_{\rm links}|0\rangle$, and then how to reduce the coupling.

Strong coupling limit: Because $\hat{H}_{\rm ind}$ contributes both to U and V in $\hat{H}_{\rm imp}$ with comparable magnitudes and $|J| \ll U$ in order to satisfy the Gauss constraint, the system will be in the strong coupling regime. For example, consider the following parameters on the link islands $E_C/E_J = 0.300$, $(E_L + 2E_L^c)/E_J = 0.015$ and $E_C^a/E_J^a = 0.200$, $(E_L^a + 4E_L^c)/E_J^a = 0.010$ on the ancilla islands. The link states $|\pm 1\rangle$ are nearly

degenerate with splitting $= 0.003E_J$. Choosing $E_L^c/E_J = 0.001$, $E_C^c/E_C = 0.600$ (by choosing $C_c = 75C$), and $E_J^a = 5E_J$ (so that $E_L^c/\Delta = 0.023$ ensuring that the perturbation theory on the ancilla is valid), we find $U/E_J = 0.032$, $V/E_J = 0.288$, and $J/U = -0.038$, which by Eq. 1 gives $g_{\rm elec}^2 g_{\rm magn}^2 \sim 3066$.

Intermediate coupling: In order to reduce the electric field term we can shift the energy of state $|0\rangle$ by off resonant coupling to an excited state $|s\rangle$ above the qutrit subspace. Consider a driving field that couples to the fluxonium at frequency ω_F which is detuned from the $|0\rangle \to |s\rangle$ transition by $\delta = \omega_F - (E_s - E_0)$. Because of the anharmonic energy spacing of the fluxonium the frequency ω_F can be chosen to be very far off resonant for transitions involving the other qutrit states. Using, e.g. inductive coupling via a quarter wavelength transmission line [36], the time dependent fluxonium-field interaction is $\hat{H}_{FF} = \frac{\Omega}{2}|s\rangle\langle 0|e^{-i\omega_F t} + h.c.$ where the Rabi frequency is $\Omega = -g\langle s|\hat{\phi}|0\rangle$ and g depends on physical parameters of the transmission line and the fluxonium [36]. If one is far detuned from other excited states, then the Hamiltonian $\hat{H}_{\rm imp}$ in the qutrit subspace is modified by the replacement $V \to V + \frac{|\Omega|^2}{4\delta}$, hence choosing $\delta < 0$ we can reduce the strength of the electric coupling. In practice there will be energy shifts accumulated from off resonant coupling to multiple excited states by all three qutrit states and one should optimize over the field frequency ω_F and strengths g to reduce the cumulative electric coupling V. Doing so for the fluxonium parameters above, the choice $|g|^2 = 0.2$ and frequency $\omega_F = 1.588E_J$ provides for $V \simeq 0$ and $g_{\rm elec}^2 g_{\rm magn}^2 \gtrsim 1$.

Now we examine the effects of decoherence on the quantum simulation. We envision starting in the gapped product state $|G(0)\rangle = \prod_{\rm links}|0\rangle$ by tuning parameters to the extremely strongly coupled regime (without driving field), and adiabatically evolving the ground state to an intermediate coupling regime. The adiabatic evolution could be done by slowly increasing the driving field Rabi frequency over a time $T_{\rm sim}$ and as described below, nonlocal order parameters can be measured as a function of final coupling strength (see Fig. 3b). As shown in Fig. 3c, the ground state $|G(t)\rangle$ is gapped throughout with energy $\Delta E_{\rm gap}(t) \sim 4g_{\rm elec}^2(t)$, and from the effective model $\hat{H}_{\rm eff}$ is minimal at $V = 0$ where $\Delta E_{\rm gap}^{\rm min} \sim 8J^2/U$. The decoherence times for fluxonium tuned to the qutrit point has been reported at $T_1 \sim T_2 \sim 50\mu$s [35]. Consider $U = 0.032E_J$ as above and choose $E_J = 40$GHz [36] and $T_{\rm sim} = 2/\Delta E_{\rm gap}^{\rm min} = 0.135\mu$s. The bit flip error time for the inverted qubit ancilla is, $T_1^a \sim 1$ms [35], giving an error rate per ancilla of $1 - e^{-T_{\rm sim}/T_1^a} \sim 10^{-4}$. Altogether, this should allow for reliable simulations on ~ 1000 link variables.

The nonlocal operators relevant to the spin-1 QLM are the Wilson loop: $\hat{W}(\mathcal{C}) = \hat{S}^+ \otimes \hat{S}^- \otimes \cdots \otimes \hat{S}^+ \otimes \hat{S}^-$, on a loop $\mathcal{C}$ on the lattice and the 't Hooft disorder operator $\hat{\Upsilon}(\phi) = e^{-i\phi\hat{S}_0^z} \otimes e^{i\phi\hat{S}_1^z} \otimes \cdots \otimes e^{-i\phi\hat{S}_{n-2}^z} \otimes e^{i\phi\hat{S}_{n-1}^z}$, where the spins are ordered on a line in the dual lattice with the first spin at location 0 on the boundary. We show how these operators can be measured on our system in a non-demolition manner. The idea is to prepare the ground state of the spin-1 lattice Hamiltonian and then turn off $\hat{H}_{\rm imp}$ and measure non local operators. Because the measurement is non-demolition, conjugate operators are not disturbed and the measured spins will generically maintain correlations with the rest of the system. If so desired, the measurement could act as a quench on the system and subsequent dynamics after the Hamiltonian is turned on again could be investigated [37].

Our mechanism for measuring the nonlocal operators involves embedding the fluxonium array in a microwave cavity and coupling a subset of spins to a single cavity mode (see Fig. 3a). Ultimately, only a single qubit degree of freedom need be measured which is particularly advantageous if measurement is a significant source of error. In contrast, if all the spins were measured independently and joint statistics collected, then the overall loss of fidelity in the operation would scale exponentially with the number of spins measured. The two ingredients we require is a dispersive coupling of spins in a region $\mathcal{R}$: $\hat{H}_{\rm int} = -\chi\hat{a}^\dagger\hat{a}\sum_{j\in\mathcal{R}}|0\rangle_j\langle 0|$ and a coupling between an ancilla A (such as one of the ancilla qubits) and the bosonic field: $\hat{H}_{\rm int}^A = -\chi\hat{a}^\dagger\hat{a}|1\rangle_A\langle 1|$ (note the two coupling strengths do not have to be equal). Here the bosonic creation and annihilation operators are $\hat{a}^\dagger$ and $\hat{a}$ satisfying $[\hat{a},\hat{a}^\dagger] = 1$. Selectively addressing cavity coupling within the region $\mathcal{R}$ or at the ancilla location could be done by coherently mapping the noninteracting spins to non interacting local states which are far detuned from the cavity coupling. In Sec. III of [33] we show two methods to measure the nonlocal operators. One method uses a geometric phase gate which only requires the ability to prepare the vacuum state of the cavity and perform a sequence of displacement operators and evolution generated by $\hat{H}_{\rm int}$. The second method can be done in a single step but requires the ability to prepare a superposition of vacuum and a single photon state of the cavity. Let the cavity decay rate be κ and model the decoherence on the spins during the measurement time t by a collective depolarization error probability $p = 1 - e^{-\gamma t}$ and an independent depolarization error at the same rate γ. The overall process fidelity for the geometric phase gate on n spins, including 1 ancilla spin, followed by measurement of the ancilla is

$$\begin{aligned} F_{\rm pro}^{(gp)}(\theta,\Omega) \;>\; & \eta_A(1 - n(4\pi + 6\theta)\gamma/|\chi|) \\ & \times\Big(1 - \tfrac{\pi\Omega\kappa}{|\chi|}(e^{-3\theta\kappa/|\chi|} + e^{-\theta\kappa/|\chi|})\big(1 + \tfrac{\pi\kappa}{2|\chi|}\big)\Big), \end{aligned} \tag{5}$$

where $\eta_A < 1$ describes finite detection fidelity of the ancilla spin. For the Wilson loop measurement $\Omega = \pi/\sqrt{3}, \theta = 2\pi/3$, while for the 't Hooft string $\hat{\phi}(\pi)$ measurement $\Omega = \pi/2, \theta = \pi/2$. For the single photon implementation the process fidelity is $F_{\rm pro}^{(sp)}(\theta) > \eta_p(1 - n(1 - e^{-\gamma\bar{t}(\theta)}))$, where $\eta_p \le 1$ describes finite single photon detection fidelity, and where the mean gate time is $\bar{t}(\theta) = ((1 + e^{2\theta\kappa/|\chi|})(2\theta)^2\kappa/|\chi|^2)/(2\theta\kappa/|\chi| + e^{2\theta\kappa/|\chi|} - 1)$. Here, for the Wilson loop measurement $\theta = 2\pi/3$, while for measurement of the 't Hooft string $\hat{\Upsilon}(\phi)$, $\theta = \phi/2$. In the presence of inhomogeneities in the dispersive coupling strength χ, the error $\mathcal{E}$ for the global gates with angle θ is $\mathcal{E} \approx \theta^2|\mathcal{R}|(|\mathcal{R}| - 1)\varepsilon^2/2$ where $\varepsilon = \max_j|(\alpha_j - \alpha)/\alpha|$ is the maximum fractional inhomogeneity (see Sec. III of [33]).

Using transmons coupled to a 3D microwave cavity [39] the following values were reported for one island: $\gamma = 66.7$kHz, $|\chi|/2\pi = 99.8$MHz,$\kappa = 22.2$kHz. Single-shot transmon qubit measurements have also been reported with up to $\eta_A = 0.919$

fidelity [40]. Assuming these parameters for fluxonium and local addressability, using the geometric phase gate a Wilson loop of length 8 or a 't Hooft string of size 10 could be measured with 90% fidelity. Given efficient single microwave photon detectors then the single photon protocol would allow for a measurement of a Wilson loop on $n-1$ spins with fidelity $F_{\rm pro}^{(sp)} > \eta_p(1-n\times 2.5\times 10^{-3})$. Distinguishability between 0 and 1 microwave photons can be achieved in a microwave cavity with up to 90% efficiency [41].

In summary, we have described how a lattice version of QED in 2+1 dimensions can be simulated using superconducting arrays of fluxonium which is tunable between strongly and intermediately coupling regimes. We have defined QLM order and disorder parameters and shown how to measure them in a non destructive manner. Beyond ground state characterization, this mechanism could also be used to probe dynamics by e.g. quenching the system and measuring how the non-local order/disorder parameters vary in time.

Acknowledgements: This work was partially supported by the ARC Centre of Excellence for Engineered Quantum Systems EQUS (Grant No CE110001013). We also acknowledge financial support from Basque Government Grants IT472-10, Spanish MINECO FIS2012-36673-C03-02, UPV/EHU Project No. EHUA15/17, UPV/EHU UFI 11/55 and SCALE-QIT EU project. G.P and D.V. acknowledge support by the ERC-St Grant ColdSIM (No. 307688), EOARD, UdS via Labex NIE and IdEX, RYSQ.

[1] K.G. Wilson. Confinement of quarks. Phys. Rev. D **10** 2445 (1974)
[2] H. J. Rothe. Lattice gauge theories, World Scientific (2012)
[3] X.G. Wen. Quantum Field Theory of Many-Body Systems: From the Origin of Sound to an Origin of Light and Electrons, Oxford Graduate Texts (2004)
[4] G. t Hooft. On the phase transition towards permanent quark confinement. Nucl. Phys., B **138** 1 (1978)
[5] H.-W. Lin and H. B. Meyer (Eds.), Lattice QCD for Nuclear Physics (Springer, Heidelberg, 2015).
[6] H. Weimer, M. Muller, I. Lesanovsky, P. Zoller, H.P. Büchler, A Rydberg quantum simulator, Nat.Phys. **6**, 382 (2010)
[7] E. Kapit, E. Mueller, Optical-lattice Hamiltonians for relativistic quantum electrodynamics, Phys. Rev. A **83**, 033625 (2011)
[8] E. Zohar, B. Reznik, Confinement and Lattice Quantum-Electrodynamic Electric Flux Tubes Simulated with Ultra-cold Atoms, Phys. Rev. Lett. **107**, 275301 (2011)
[9] J. Casanova, L. Lamata, I.L. Egusquiza, R. Gerritsma, C. F. Roos, J. J. Garcia-Ripoll, E. Solano, Quantum Simulation of Quantum Field Theories in Trapped Ions, Phys. Rev. Lett. **107**, 260501 (2011)
[10] E. Zohar, J.I. Cirac, B. Reznik, Simulating Compact Quantum Electrodynamics with Ultracold Atoms: Probing Confinement and Non-perturbative Effects, Phys. Rev. Lett. **109**, 125302 (2012)
[11] D. Banerjee, M. Dalmonte, M. Muller, E. Rico, P. Stebler, U.-J. Wiese, P. Zoller, Atomic Quantum Simulation of Dynamical Gauge Fields Coupled to Fermionic Matter: From String Breaking to Evolution after a Quench, Phys. Rev. Lett. **109**, 175302 (2012)
[12] E. Zohar, J.I. Cirac, B. Reznik, Simulating (2+1)-Dimensional Lattice QED with Dynamical Matter Using Ultracold Atoms, Phys. Rev. Lett. **110**, 055302 (2013)
[13] P. Hauke, D. Marcos, M. Dalmonte, P. Zoller, Quantum Simulation of a Lattice Schwinger Model in a Chain of Trapped Ions, Phys. Rev. X **3**, 041018 (2013)
[14] L. Tagliacozzo, A. Celi, A. Zamora, M. Lewenstein, Optical Abelian lattice gauge theories, Ann. Phys. **330**, 160 (2013)
[15] E. Zohar, J.I. Cirac, B. Reznik, Quantum simulations of gauge theories with ultracold atoms: Local gauge invariance from angular-momentum conservation, Phys. Rev. A **88**, 023617 (2013)
[16] K. Stannigel, P. Hauke, D. Marcos, M. Hafezi, S. Diehl, M. Dalmonte, P. Zoller, Constrained Dynamics via the Zeno Effect in Quantum Simulation: Implementing Non-Abelian Lattice Gauge Theories with Cold Atoms, Phys. Rev. Lett. **112**, 120406 (2014)
[17] A.W. Glaetzle, M. Dalmonte, R. Nath, I. Rousochatzakis, R. Moessner, P. Zoller, Quantum Spin-Ice and Dimer Models with Rydberg Atoms, Phys. Rev. X **4**, 04103715 (2014)
[18] S. Notarnicola, E. Ercolessi, P. Facchi, G. Marmo, S. Pascazio, F.V. Pepe, Discrete Abelian Gauge Theories for Quantum Simulations of QED, arXiv:1503.04340
[19] A. Bazavov, Y. Meurice, S.-W. Tsai, J. Unmuth-Yockey, J. Zhang, Gauge-invariant implementation of the Abelian Higgs model on optical lattices, arXiv:1503.08354
[20] A. Bermudez, D. Porras, Interaction-Dependent Photon-Assisted Tunneling in Optical Lattices: A Quantum Simulator of Strongly-Correlated Electrons and Dynamical Gauge Fields, New J. Phys. **17** 103021 (2015)
[21] D. Marcos, P. Rabl, E. Rico, P. Zoller, Superconducting Circuits for Quantum Simulation of Dynamical Gauge Fields, Phys. Rev. Lett. **111**, 110504 (2013)
[22] D. Marcos, P. Widmer, E. Rico, M. Hafezi, P. Rabl, U.-J. Wiese, P. Zoller, Two-dimensional lattice gauge theories with superconducting quantum circuits, Ann. Phys. **351**, 634 (2014)
[23] L. Garcia-Alvarez, J. Casanova, A. Mezzacapo, I.L. Egusquiza, L. Lamata, G. Romero, E. Solano, Fermion-Fermion Scattering in Quantum Field Theory with Superconducting Circuits, Phys. Rev. Lett. **114**, 070502 (2015)
[24] A. Mezzacapo, E. Rico, C. Sabin, I. L. Egusquiza, L. Lamata, E. Solano, Non-Abelian Lattice Gauge Theories in Superconducting Circuits, Phys. Rev. Lett. **115**, 240502 (2015)
[25] U.-J. Wiese, Towards quantum simulating QCD, Nucl. Phys. A **931**, 246 (2014).
[26] E. Zohar, J.I. Cirac, B. Reznik, Quantum Simulations of Lattice Gauge Theories using Ultracold Atoms in Optical Lattices, arXiv:1503.02312 (2015).
[27] J. Kogut and L. Susskind. Hamiltonian formulation of Wilsons lattice gauge theories. Phys. Rev. D **11** 395 (1975)
[28] A.M. Polyakov. Gauge Fields and Strings. Harwood Academic Publishers (London), (1987)
[29] D. Horn. Finite matrix models with continuous local gauge invariance. Phys. Lett. B, **100**, 149 (1981)
[30] P. Orland, D. Rohrlich. Lattice gauge magnets: Local isospin from spin. Nucl. Phys. B, **338**, 647 (1990)
[31] S. Chandrasekharan, U-J. Wiese. Quantum link models: A discrete approach to gauge theories. Nucl. Phys. B, **492**, 455

(1997)
[32] D.S. Rokhsar, S.A. Kivelson. Superconductivity and the Quantum Hard-Core Dimer Gas. Phys. Rev. Lett. **61**, 2376 (2009)
[33] See supplemental information.
[34] S.M. Girvin. Superconducting Qubits and Circuits: Artificial Atoms Coupled to Microwave Photons. In: Lecture Notes delivered at Les Houches Summer School, July 2011. to be published by Oxford University Press.
[35] I.M. Pop, K. Geerlings, G. Catelani, R.J. Schoelkopf, L.I. Glazman, M.H. Devoret. Coherent suppression of electromagnetic dissipation due to superconducting quasiparticles. Nature **508** 369 (2014).
[36] N.A. Masluk, Reducing the losses of the fluxonium artificial atom, PhD Thesis Yale (2012).
[37] It was proven in Ref.[38] that non-demolition measurements of space like non-Abelian Wilson loops are not physical because they would allow for faster than light signaling. However, Abelian Wilson loops such as considered here have no such obstruction provided the spins on the loop have access to a shared entanglement resource which here is the common cavity mode.
[38] D. Beckman, D. Gottesman, A. Kitaev, and J. Preskill. Measurability of Wilson loop operators. Phys. Rev. D **65**, 065022 (2002).
[39] H. Paik, D.I. Schuster, L.S. Bishop, G. Kirchmair, G. Catelani, A. P. Sears, B.R. Johnson, M.J. Reagor, L. Frunzio, L.I. Glazman, S.M. Girvin, M.H. Devoret, R.J. Schoelkopf. Observation of High Coherence in Josephson Junction Qubits Measured in a Three-Dimensional Circuit QED Architecture. Phys. Rev. Lett. **107**, 240501 (2011).
[40] Y. Liu, S. Srinivasan, D. Hover, S. Zhu, R. McDermott, A.A. Houck. High fidelity single-shot readout of a transmon qubit using a SLUG micro-wave amplifier. arXiv:1401.5184 (2014).
[41] S. R. Sathyamoorthy, L. Tornberg, A. F. Kockum, B.Q. Baragiola, J. Combes, C.M. Wilson, T. M. Stace, and G. Johansson, Phys. Rev. Lett. **112**, 093601 (2014).
[42] A.M. Rey, G. Pupillo, C.W. Clark, C.J. Williams. Ultracold atoms confined in an optical lattice plus parabolic potential: A closed-form approach. Phys. Rev. A **72**, 033616 (2005).
[43] L. Jiang, G. K. Brennen, A. V. Gorshkov, K. Hammerer, M. Hafezi, E. Demler, M. D. Lukin, P.Zoller, Nature Phys. **4**, 482 (2008)
[44] G. K. Brennen, K. Hammerer, L. Jiang, M. D. Lukin, P.Zoller, arXiv:0901.3920.

Supplemental Information

I. LARGE-N REPRESENTATION OF THE $U(1)$ QLM AND DUALITY TRANSFORMATION

The local Hilbert space in a $U(1)$ QLM is bounded and finite, i.e., $\mathcal{H}_{x,x+\mu_x} = \mathbb{C}^{N+1} = \{|E_{x,x+\mu}\rangle\}$, with $|E_{x,x+\mu}| \leq \frac{N}{2}$ and $N \in \mathbb{Z}$. In this local Hilbert space, we redefine the local operators, such that

$$\begin{aligned}
&\hat{E}_{x,x+\mu}|E_{x,x+\mu}\rangle = E_{x,x+\mu}|E_{x,x+\mu}\rangle;\\
&\hat{W}_{x,x+\mu_x} = \frac{\hat{U}_{x,x+\mu_x}}{\sqrt{\frac{N}{2}\left(\frac{N}{2}+1\right)}}, \quad \hat{W}_{x,x+\mu_x}|E_{x,x+\mu}\rangle = \sqrt{\frac{\frac{N}{2}+1-E_{x,x+\mu}}{\frac{N}{2}+1}}\sqrt{\frac{\frac{N}{2}+E_{x,x+\mu}}{\frac{N}{2}}}|E_{x,x+\mu}-1\rangle;\\
&\hat{W}^{\dagger}_{x,x+\mu_x} = \frac{\hat{U}^{\dagger}_{x,x+\mu_x}}{\sqrt{\frac{N}{2}\left(\frac{N}{2}+1\right)}}, \quad \hat{W}^{\dagger}_{x,x+\mu_x}|E_{x,x+\mu}\rangle = \sqrt{\frac{\frac{N}{2}+1+E_{x,x+\mu}}{\frac{N}{2}+1}}\sqrt{\frac{\frac{N}{2}-E_{x,x+\mu}}{\frac{N}{2}}}|E_{x,x+\mu}+1\rangle;
\end{aligned}$$

that fulfill the commutation relations

$$\begin{aligned}
&\left[\hat{W}^{\dagger}_{x,x+\mu_x}, \hat{W}_{y,y+\mu_y}\right] = \delta_{x,y}\frac{2\hat{E}_{x,x+\mu}}{\frac{N}{2}\left(\frac{N}{2}+1\right)};\\
&\left[\hat{E}_{x,x+\mu}, \hat{W}_{x,x+\mu_x}\right] = -\hat{W}_{x,x+\mu_x}
\end{aligned} \tag{6}$$

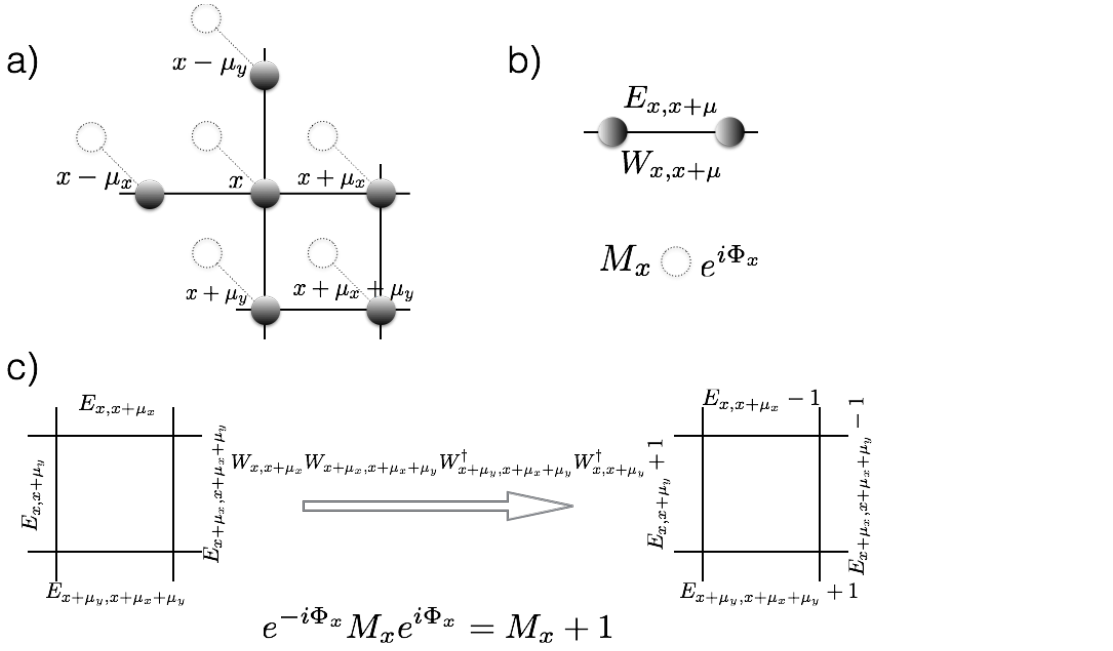

FIG. 4. a) Direct and dual lattice structure. b) Local degrees of freedom on the direct and dual models. c) Action of the plaquette operator on the direct and dual formulation.

A. Large-N Hamiltonian

With the operators, we can define a large-N Hamiltonian

$$\hat{\tilde{H}} = \hat{H}_{\text{elec}} + \hat{\tilde{H}}_{\text{magn}} = g^2_{\text{elec}}\sum_{x,\mu}\left(\hat{E}_{x,x+\mu}\right)^2 - \frac{1}{\tilde{g}^2_{\text{magn}}}\sum_{x,\mu_x,\mu_y}\left(\hat{W}_{x,x+\mu_x}\hat{W}_{x+\mu_x,x+\mu_x+\mu_y}\hat{W}_{x+\mu_x+\mu_y,x+\mu_y}\hat{W}_{x+\mu_y,x} + \text{h.c.}\right), \tag{7}$$

that is equivalent to Eq. (1) if $g_{\rm magn} = \tilde{g}_{\rm magn}\left[\frac{N}{2}\left(\frac{N}{2}+1\right)\right]^2$. In the limit $\langle \hat{E}_{x,x+\mu}\rangle \ll N$, the commutator of the links operators behaves as $\left[\hat{W}^\dagger_{x,x+\mu_x}, \hat{W}_{y,y+\mu_y}\right] \to 0$ and we recover the Wilson limit.

In this representation, it is instructive to study the model defining the basic local degrees of freedom as "plaquette" variables, $e^{-i\hat{\Phi}_x} = \hat{W}_{x,x+\mu_x}\hat{W}_{x+\mu_x,x+\mu_x+\mu_y}\hat{W}_{x+\mu_x+\mu_y,x+\mu_y}\hat{W}_{x+\mu_y,x}$. Due to the previous commutation relations, in the large-N limit, these local variables can be treated as independent. In addition to this, the operators given by 't Hooft strings, connecting a given plaquette with a reference one at infinity, correspond to local creation or annihilation operators on that plaquette. A complete description of the local "dual" Hilbert space and the dual Hamiltonian is the task of the next section.

B. Dual Hamiltonian in the large-N limit

In what follows, we define the local dual Hilbert space and dual degrees of freedom, local dual operators, and the dual Hamiltonian dynamics of a $U(1)$ quantum link model in $2+1$ dimensions.

The local degrees of freedom are vortices located on every plaquette x of the initial lattice. In the dual lattice the operator $e^{-i\hat{\Phi}_x} = \hat{W}_{x,x+\mu_x}\hat{W}_{x+\mu_x,x+\mu_x+\mu_y}\hat{W}_{x+\mu_x+\mu_y,x+\mu_y}\hat{W}_{x+\mu_y,x}$, that measure the magnetic flux through a plaquette, is a local operator.

Due to the Gauss' law around every vertex, there is a conservation of the total electric flux, i.e., $E_{x-\mu_x,x} + E_{x-\mu_y,x} = E_{x,x+\mu_x} + E_{x,x+\mu_y}$. It is fairly simple to realize that this relation is automatically satisfied if we define dual variables M_x placed on the middle of the plaquette of the direct lattice (or on the sites of the dual lattice) such that:

$$\hat{E}_{x,x+\mu_y} = \hat{M}_{x+\mu_y} - \hat{M}_{x+\mu_x+\mu_y};\;\; \hat{E}_{x,x+\mu_x} = \hat{M}_{x+\mu_x+\mu_y} - \hat{M}_{x+\mu_x};\;\; \hat{E}_{x-\mu_y,x} = \hat{M}_x - \hat{M}_{x+\mu_x};\;\; \hat{E}_{x-\mu_x,x} = \hat{M}_{x+\mu_y} - \hat{M}_x. \tag{8}$$

The solution of the dual variables in terms of the electric fluxes, reveals the variables $\hat{M}_x$ as the generators of the 't Hooft strings, i.e. $\hat{M}_x = \sum_{n=0}^{\infty}\hat{E}_{x-\mu_y+n\mu_x,x+n\mu_x}$ In fact this dual variable and the magnetic flux are conjugate variables, fulfilling: $[\hat{M}_x, e^{\pm i\hat{\Phi}_x}] = \pm e^{\pm i\hat{\Phi}_x}$.

With this change of variables, the dual Hamiltonian can be recast into

$$\hat{H} = g^2_{\rm elec}\sum_{x,\mu}\left[\hat{M}_x - \hat{M}_{x+\mu}\right]^2 - \frac{1}{\tilde{g}^2_{\rm magn}}\sum_x\left[e^{i\hat{\Phi}_x} + e^{-i\hat{\Phi}_x}\right]. \tag{9}$$

This Hamiltonian is invariant under the unitary transformation $e^{i2\pi\sum_x \alpha_x\hat{M}_x}$ with $\alpha_x \in \mathbb{Z}$. Then, the spectrum of this Hamiltonian is periodic in Φ_x with a period 2π and the eigenfunctions $|\psi\rangle$ are Bloch's functions.

To analyze the behavior of this Hamiltonian, we study two limits $g^2_{\rm elec}\tilde{g}^2_{\rm magn} \gg 1$ and $g^2_{\rm elec}\tilde{g}^2_{\rm magn} \ll 1$. In the strong coupling limit $g^2_{\rm elec}\tilde{g}^2_{\rm magn} \gg 1$, the Hamiltonian reduces to $\hat{H} \to g^2_{\rm elec}\sum_{x,\mu}\left[\hat{M}_x - \hat{M}_{x+\mu}\right]^2$, the eigenfunctions are eigenstates of the dual potential $\hat{M}_x$ that can be written as plane-waves in the magnetic flux basis, i.e., $\hat{M}_x|m_x\rangle = m_x|m_x\rangle$, $|m_x\rangle = \frac{1}{\sqrt{2\pi}}\int_{-\pi}^{\pi} d\phi_x\; e^{i\phi_x m_x}|\phi_x\rangle$. In the weak coupling limit $g^2_{\rm elec}\tilde{g}^2_{\rm magn} \ll 1$, and the Hamiltonian reduces to $\hat{H} \to -\frac{1}{\tilde{g}^2_{\rm magn}}\sum_x\left[e^{i\hat{\Phi}_x} + e^{-i\hat{\Phi}_x}\right]$.

From this duality exercise, we can realize that the previous gauge invariant $U(1)$ quantum link model is dual in the large-N limit to a bosonic model with a global $U(1)$ invariance where the local degrees of freedom are magnetic vortices of the initial one. Hence, a possible phase transition in the gauge model is recast in a transition of the model with the global symmetry where the order parameter is given by the 't Hooft strings. The order phase corresponds to the confined phase, while the disorder phase in the global theory maps to a deconfined phase in the gauge theory.

II. DETAILS ON THE IMPLEMENTATION WITH FLUXONIA

A. Local Hilbert space and the tight binding limit

In a first case, we assume that the local inductive energy is negligible with respect to the local capacitive or the Josephson energies. The Hamiltonian for the fluxonium at link k can be written $\hat{H}_k = \hat{H}^J_k + \frac{E_L}{2}\hat{\phi}^2_k$ where $\hat{H}^J_k = -4E_C\frac{\partial^2}{\partial\hat{\phi}^2_k} - E_J\cos(\hat{\phi}_k)$. In the tight binding limit, where the lattice wells are deep enough such that the particle dynamics is restricted to nearest neighbor only hoping, then one can find simplified expressions for the lowest energy eigenstates and eigenfunctions (see Ref. [42]). For $E_L \ll E_J$ the lowest energy states $w_0(\phi_k - 2\pi m_k)$ are the first band Wannier function with a well defined magnetic flux $2\pi m_k$. For deep lattices we can approximate the Wannier functions as ground state harmonic oscillators whose wave-functions are approximately

$$w_0(\phi_k - 2\pi m_k) = \frac{1}{(\pi\sigma^2)^{1/4}}e^{-(\phi_k - 2\pi m_k)^2/2\sigma^2}.$$

where

$$\sigma = \left(\frac{8E_C}{E_J}\right)^{1/4},$$

is standard deviation of the wave-function localized at the potential minima $2\pi m$, $m_{\alpha,\beta} \in \mathbb{Z}$. The gap to the second energy band is of the order $\hbar\omega_0 \sim \sqrt{8E_C E_J} = \sigma^2 E_J$ and the matrix elements of the Hamiltonian $\hat{H}^J_{\alpha,\beta}$ in this basis is:

$$\langle m'_k|\hat{H}^J_k|m_k\rangle = E_J e^{-\pi^2\left(m'_k-m_k\right)^2/\sigma^2}\left\{\frac{\sigma^2}{4} - \frac{\pi^2\left(m'_k-m_k\right)^2}{2} - e^{-\sigma^2/4}\cos\left[\pi(m'_k+m_k)\right]\right\}, \tag{10}$$

and then the hoping rate t between nearest neighbor wells is:

$$t = E_J e^{-\pi^2/\sigma^2}\left(\frac{\sigma^2}{4} - \frac{\pi^2}{2} + e^{-\sigma^2/4}\right) \tag{11}$$

The *tight binding limit* is determined by the condition $\sigma^2 E_J \gg |t|$ in which case we are justified in projecting onto the lowest energy level on the minimum of the cosine potential. This inequality is always fulfilled with the gaussian approximation. For instance, tunneling has a local extremum at $\sigma \sim 3.168$ where $t \sim -0.877E_J$ and $\frac{\hbar\omega_0}{|t|} \sim 11.446$. In addition to this, the fact that we choose the minima at locations $\phi = 2\pi m$ and all with the same standard deviation is valid only when the quadratic potential is a weak perturbation to the lattice, $E_L \ll E_C \leq E_J$.

B. Ancilla mediated inductive coupling for Gauss' Law constraint

Consider the interactions between link fluxonia which are inductively coupled pairwise, with energy E^c_L, to a single ancillary fluxonium a located at a vertex v. The ancilla has an offset flux such that the lowest energy states define a qubit mode while for the links the low energy states define a qutrit. The Hamiltonian for this system is

$$\hat{H}_{\text{vertex}} = \hat{H}_a + \sum_{k\in\mathcal{N}(v)}\hat{H}_k + \frac{E^c_L}{2}\sum_{k\in\mathcal{N}(v)}(\hat{\phi}_a - \hat{\phi}_k)^2 = \hat{H}'_a + \sum_{k\in\mathcal{N}(v)}\hat{H}'_k - E^c_L\hat{\phi}_a\sum_{k\in\mathcal{N}(v)}\hat{\phi}_k, \tag{12}$$

where $\mathcal{N}(v)$ denotes the set of links in neighborhood of the vertex v. Here $\hat{H}_a = E_e|e\rangle\langle e| + E_g|g\rangle\langle g|$ is the local ancilla Hamiltonian and $\hat{H}_k$ is the local link Hamiltonian without contributions from the inductive interaction. The local Hamiltonians including the energy shifts due to the inductive couplings and assuming a square lattice with $|\mathcal{N}(v)| = 4$ are

$$\begin{aligned}
\hat{H}'_a &= (E_e + 2E^c_L\langle e|\hat{\phi}^2_a|e\rangle)|e\rangle\langle e| + (E_g + 2E^c_L\langle g|\hat{\phi}^2_a|g\rangle)|g\rangle\langle g|,\\
\hat{H}'_k &= \hat{H}_k + \frac{E^c_L}{2}\sum_{\{m_k\}}\langle\hat{\phi}^2_k\rangle_{m_k}|m_1m_2m_3m_4\rangle\langle m_1m_2m_3m_4|.
\end{aligned}$$

Define the ancilla energy splitting $\Delta = [(E_e + 2E^c_L\langle e|\hat{\phi}^2_a|e\rangle) - (E_g + 2E^c_L\langle g|\hat{\phi}^2_a|g\rangle)] > 0$. Let's focus on the interaction part of the Hamiltonian. We transform to an interaction picture defined by H'_a, so that

$$H_I(t) = -E^c_L\phi_a(t)\sum_{k\in\mathcal{N}(v)}\hat{\phi}_k, \tag{13}$$

where $\hat{\phi}_a(t) = e^{i\hat{H}'_a t}\hat{\phi}_a e^{-i\hat{H}'_a t}$. To calculate the effective Hamiltonian induced by the ancilla, we need to expand the unitary evolution operator generated by $\hat{H}_I(t)$ to second order, project into the excited state $|e\rangle$ of the ancilla, and find the terms that increase linearly in t. The reason for projecting onto $|e\rangle$ for the ancilla rather than $|g\rangle$ is to arrive at the correct sign for the effective interaction as we show below. Specifically,

$$\begin{aligned}
\hat{U}_{\text{eff}}(t) &= \text{Tr}_a\hat{U}(t) = \text{Tr}_a\mathcal{T}e^{-i\int_0^t dt\,\hat{H}_I(t)}\\
&\approx \langle e|\left(1 - i\int_0^t dt_1\,\hat{H}_I(t_1) - \int_0^t dt_1\int_0^{t_1} dt_2\,\hat{H}_I(t_1)\hat{H}_I(t_2)\right)|e\rangle,\\
&\equiv 1 - i\hat{H}_{\text{eff}}t,
\end{aligned}$$

where the last line defines $\hat{H}_{\text{eff}}$. Because the ancilla qubit states are eigenstates of the parity operator defined by $P\hat{\phi} = -\hat{\phi}$, we have $\langle e|\hat{\phi}|e\rangle = 0$, so the first order term is zero. Furthermore, as the inductive interaction is diagonal in the phase operator, coupling

between different eigenstates $|m\rangle$ is exponentially suppressed. For example, in the tight binding limit, $|\langle 1|\hat{\phi}|0\rangle|/|\langle 1|\hat{\phi}|1\rangle| = e^{-\pi^2/\sigma^2}/2$. Hence the effective Hamiltonian is well approximated as diagonal in the $|m\rangle$ basis:

$$\begin{aligned}
-i\langle m_1m_2m_3m_4|\hat{H}_{\text{eff}}|m_1m_2m_3m_4\rangle t &= -\langle e|\langle m_1m_2m_3m_4|\int_0^t dt_1\int_0^{t_1} dt_2\, H_I(t_1)|g\rangle|m_1m_2m_3m_4\rangle\langle g|\langle m_1m_2m_3m_4|H_I(t_2)|e\rangle|m_1m_2m_3m_4\rangle,\\
&= -\int_0^t dt_1\int_0^{t_1} dt_2\,\langle e|\langle m_1m_2m_3m_4|H_I(t_1)|g\rangle|m_1m_2m_3m_4\rangle\langle g|\langle m_1m_2m_3m_4|H_I(t_2)|e\rangle|m_1m_2m_3m_4\rangle,\\
&= -E_L^{c2}\int_0^t dt_1\int_0^{t_1} dt_2\, e^{i\Delta t_1}e^{-i\Delta t_2}|\langle g|\phi_a|e\rangle|^2|\langle m_1m_2m_3m_4|\sum_{k\in\mathcal{N}(v)}\hat{\phi}_k|m_1m_2m_3m_4\rangle)|^2\\
&\approx -i\frac{E_L^{c2}}{\Delta}|\langle g|\phi_a|e\rangle|^2|\langle m_1m_2m_3m_4|\sum_{k\in\mathcal{N}(v)}\hat{\phi}_k|m_1m_2m_3m_4\rangle|^2 t,
\end{aligned}$$

where we assume $t \gg 1/\Delta$, which is the appropriate regime for the effective Hamiltonian to make sense. This then gives us the following Hamiltonian around the vertex:

$$\hat{H}_{\text{vertex}} = \hat{H}'_a + \textstyle\sum_{k\in\mathcal{N}(v)}\hat{H}'_k + \frac{E_L^{c2}|\langle g|\hat{\phi}_a|e\rangle|^2}{\Delta}\sum_{\{m_k\}}(\langle\hat{\phi}_1\rangle_{m_1}+\langle\hat{\phi}_2\rangle_{m_2}+\langle\hat{\phi}_3\rangle_{m_3}+\langle\hat{\phi}_4\rangle_{m_4})^2|m_1m_2m_3m_4\rangle\langle m_1m_2m_3m_4|. \tag{14}$$

In particular for a spin-1 encoding

$$\hat{H}_{\text{vertex}} = \hat{H}'_a + \sum_{k\in\mathcal{N}(v)}\hat{H}'_k + \frac{E_L^{c2}|\langle g|\hat{\phi}_a|e\rangle|^2|\langle\hat{\phi}\rangle_{m=1}|^2}{\Delta}(\sum_{k\in\mathcal{N}(v)}\hat{S}_k^z)^2,$$

where we have used the fact that the expectation values satisfy $\langle\hat{\phi}\rangle_{m=1} = \langle\hat{\phi}\rangle_{m=-1}$ and $\langle\hat{\phi}\rangle_{m=0} = 0$. On a square lattice, every link has contributions from interactions between two ancilla located at the vertices on the boundaries of the link. Hence the net effect of the modification of the local link terms is to make the replacement: $E_L \to E_L + 2E_L^c$ and on the local ancilla: $E_L^a \to E_L^a + 4E_L^c$.

Once we have the two previous ingredients: local Hilbert space spanned by well-defined magnetic fluxes and the local constraint that imposes zero flux on every vertex, any perturbative dynamics on this Hilbert space will be gauge invariant. We stress, once again, that the gap between the subspace with well-defined magnetic flux states and higher energy band is of order $\hbar\omega_0 \sim \sqrt{8E_CE_J} = \sigma^2 E_J$.

C. Capacitive interaction

Consider a square lattice with nodes at the midpoints of the edges, as in Fig.1a. Suppose each node has capacitance to ground of C, and a capacitance C_c to each of the neighboring nodes. The kinetic energy is

$$T = \sum_{\vec{r}}\left(\frac{C}{2}\dot{\phi}_{\vec{r}}^2 + \sum_{\vec{j}_{\vec{r}}}\frac{C_c}{2}(\dot{\phi}_{\vec{r}} - \dot{\phi}_{\vec{j}_{\vec{r}}})^2\right), \tag{15}$$

where the sum over $\vec{j}_{\vec{r}}$ is restricted to the 4 neighbors of node $\vec{r}$, and $\vec{r}, \vec{j}_{\vec{r}}$ are vectors in the 2D lattice.

The conjugate charge is

$$q_{\vec{r}} = \partial_{\dot{\phi}_{\vec{r}}}T = (C+4C_c)\dot{\phi}_r - C_c\sum_{\vec{j}_{\vec{r}}}\dot{\phi}_{\vec{j}_{\vec{r}}}, \tag{16}$$

This implicitly defines the capacitance matrix $\mathbf{C}$ through $\vec{q} = \mathbf{C}\vec{\phi}$ where $\vec{q}(\vec{\phi})$ is the vector of charge(flux) degrees of freedom at the lattice points. Then we write the kinetic term as

$$T = \frac{1}{2}\dot{\vec{\phi}}^T\mathbf{C}\vec{\phi} = \frac{1}{2}\vec{q}^T\mathbf{C}^{-1}\vec{q}. \tag{17}$$

Let's assume an $N_x \times N_y$ lattice with unit lattice spacing and periodic boundaries so that any lattice point can be indexed by an integer pair $\vec{r} = (r_x, r_y) \in \mathbb{Z}_{N_x} \times \mathbb{Z}_{N_y}$. The corrections to these results for lattices with open boundaries will scale like the inverse of the system size. The capacitance matrix can then be written

$$\mathbf{C} = (C+4C_c)\mathbf{1}_{N_xN_y} - C_c((X_{N_x}+X_{N_x}^\dagger)\otimes\mathbf{1}_{N_y} + \mathbf{1}_{N_x}\otimes(X_{N_y}+X_{N_y}^\dagger)),$$

where the increment operator $X_N = \sum_{j=0}^{N-1} |j+1\rangle\langle j|$. This can easily be diagonalized by a Fourier transform $F_N = \frac{1}{N}\sum_{j,k=0}^{N-1} e^{i2\pi jk/N}|j\rangle\langle k|$ as

$$F_{N_x}\otimes F_{N_y}\mathbf{C}F_{N_x}^\dagger\otimes F_{N_y}^\dagger = \sum_{n_x=0}^{N_x-1}\sum_{n_y=0}^{N_y-1} D(\vec{k})|n_x,n_y\rangle\langle n_x,n_y|.$$

where $D(\vec{k}) = (C+4C_c) - 2C_c(\cos(k_x)+\cos(k_y))$ and the momentum vectors are $\vec{k} = (k_x,k_y) = (\frac{2\pi n_x}{N_x}, \frac{2\pi n_y}{N_y})$ where $(n_x,n_y)\in \mathbb{Z}_{N_x}\times\mathbb{Z}_{N_y}$. The inverse of the capacitance matrix is then

$$\mathbf{C}^{-1} = F_{N_x}^\dagger\otimes F_{N_y}^\dagger \sum_{n_x=0}^{N_x-1}\sum_{n_y=0}^{N_y-1}\frac{|n_x,n_y\rangle\langle n_x,n_y|}{D(\vec{k})}F_{N_x}\otimes F_{N_y}.$$

and the kinetic energy is therefore,

$$T = \frac{1}{2}\sum_{\vec{r},\vec{j}} c_{\vec{r},\vec{j}}q_{\vec{r}}^* q_{\vec{j}}, \tag{18}$$

where

$$\begin{aligned} c_{\vec{r},\vec{j}} &= \langle r_x,r_y|F_{N_x}^\dagger\otimes F_{N_y}^\dagger\big[\textstyle\sum_{n_x=0}^{N_x-1}\sum_{n_y=0}^{N_y-1}\frac{|n_x,n_y\rangle\langle n_x,n_y|}{D(\vec{k})}\big]F_{N_x}\otimes F_{N_y}|j_x,j_y\rangle \\ &= \tfrac{1}{N_xN_y}\textstyle\sum_{n_x=0}^{N_x-1}\sum_{n_y=0}^{N_y-1}\frac{e^{i\vec{k}\cdot(\vec{r}-\vec{j})}}{D(\vec{k})}. \end{aligned}$$

In the large square lattice size limit $N_x \simeq N_y \to \infty$, for a separation between lattice sites $\Delta\vec{x}$

$$c(\Delta\vec{x}) = \frac{1}{(2\pi)^2}\int_0^{2\pi}dk_x\int_0^{2\pi}dk_y\frac{e^{i\vec{k}\cdot\Delta\vec{x}}}{D(\vec{k})}. \tag{19}$$

Defining the quantity $\xi = \sqrt{C_c/C}$, the on-site interaction is

$$c(0) = \frac{1}{C}\frac{2K\Big(-\frac{16\xi^2}{(\xi^{-2}+8)}\Big)}{\pi\xi\sqrt{\xi^{-2}+8}} \tag{20}$$

where $K(x)$ is the elliptic integral of the first kind. In the limit $C_c\to 0$, $c(0) = 1/C$ as expected. For $|\Delta\vec{x}|>0$ the non oscillatory support of the integrand is for $k\ll 1$ so we can expand the denominator as $D(\vec{k})\approx C\xi^2(k^2+\xi^{-2})$,

$$\begin{aligned} c(|\Delta\vec{x}|>0) &\simeq \tfrac{1}{C}\tfrac{1}{(2\pi\xi)^2}\textstyle\int_0^{2\pi}dkk\int_0^{2\pi}d\theta\frac{e^{ik|\Delta\vec{x}|\cos(\theta)}}{k^2+\xi^{-2}} \\ &= \tfrac{1}{C}\tfrac{1}{2\pi\xi^2}\textstyle\int_0^{2\pi}dkk\frac{J_0(k|\Delta\vec{x}|)}{k^2+\xi^{-2}} \\ &= \tfrac{1}{C}\tfrac{1}{2\pi\xi^2}K_0(|\Delta\vec{x}|/\xi). \end{aligned} \tag{21}$$

where $J_0(x)$ is the zeroth Bessel function of the first kind and $K_0(x)$ is the modified zeroth Bessel function of the second kind. The parameter ξ plays the role of a correlation length. For $|\Delta\vec{x}|/\xi\gg 1$, the interaction strength due to capacitive coupling between superconducting islands falls off exponentially with island separation $c(|\Delta\vec{x}|)\simeq\frac{1}{C}\sqrt{\frac{1}{8\pi|\Delta\vec{x}|/\xi}}\frac{e^{-|\Delta\vec{x}|/\xi}}{\xi^2}$. For short separations satisfying $|\Delta\vec{x}|/\xi\ll 1$, $c(|\Delta\vec{x}|)\simeq -\frac{\ln(|\Delta\vec{x}|/2\xi)+\gamma}{2\pi\xi^2}$, where $\gamma\approx 0.5772$ is the Euler gamma constant.

Under quantization of the charge degree of freedom $q_{\vec{r}}\to 2e\hat{n}_{\vec{r}}$ where e is the electron charge and $\hat{n}_{\vec{r}}$ is the number operator for the Cooper pairs at the island at site $\vec{r}$, the kinetic energy operator is

$$T = 4E_C\sum_{\vec{r}}\hat{n}_{\vec{r}}^2 + 8E_C^c\sum_{\langle\vec{j},\vec{r}\rangle}\hat{n}_{\vec{j}}\hat{n}_{\vec{r}} + 4E_C\sum_{\vec{j},\vec{r};|\vec{j}-\vec{r}|>1}\frac{c(|\vec{j}-\vec{r}|)}{c(0)}\hat{n}_{\vec{j}}\hat{n}_{\vec{r}}, \tag{22}$$

where the on site energy $E_C = \frac{e^2}{2C}$, and the nearest neighbor coupling magnitude is $E_C^c = E_C\frac{c(1)}{c(0)}\simeq E_C\frac{\sqrt{8+\xi^{-2}}K_0(\xi^{-1})}{4\xi K(-16\xi^2/(8+\xi^{-2}))}$. The factor of two in the nearest neighbour term relative to the other terms is due to the fact that we are only count the interaction between the pair on a link once. Longer range interactions in the third term fall off exponentially with separation distance as described above. The matrix elements of the kinetic energy operator for between nearest neighbor islands are computed by taking the wavefunction overlaps of the charge operator in the local eigenbasis of fluxonium. In the tight binding limit we find:

$$\langle m_k'|\hat{n}_k|m_k\rangle = \frac{i}{\sigma^2}\pi\left(m_k'-m_k\right)e^{-\pi^2\left(m_k'-m_k\right)^2/\sigma^2}. \tag{23}$$

D. Beyond tight binding limit: numerical calculation of local link eigenenergies and eigenfunctions

We wish to provide expressions for the interaction matrix elements that are valid even beyond the tight binding limit. This requires solving for the band structure for the Hamiltonian $\hat{H}_k$. First consider the local Hamiltonian with only the quadratic potential due to the inductance energy: $\hat{H}_k^L = -4E_C\frac{\partial^2}{\partial\phi_k^2} + \frac{E_L}{2}\hat{\phi}_k^2$. The eigenstates and eigenfunctions are then simply those for a harmonic oscillator with origin of potential at $\phi_k = 0$. Specifically, the eigenstates are labelled by $n \in \mathbb{N}$ with energies $E_n = \hbar\omega(n+\frac{1}{2})$, where $\hbar\omega = \sqrt{8E_LE_C}$, and the eigenfunctions are

$$\psi_n(\phi_k) = \frac{1}{\sqrt{2^n n!\sqrt{\pi}\beta}} e^{-\phi_k^2/(2\beta^2)} H_n(\phi_k/\beta),$$

where $\beta = (8E_C/E_L)^{1/4}$, and $H_n(x)$ is the n-th Hermite polynomial. The Josephson term in the potential can then be computed in this basis. When the offset flux is set to $\phi_{\text{off}} = 0$ the matrix elements are

$$-E_J\langle\psi_m(\phi_k)|\cos(\hat{\phi}_k)|\phi_n(\phi_k)\rangle = -E_J\tfrac{1}{\sqrt{2^{n+m}n!m!}}2^{\min_{n,m}}(\min_{n,m})!(-1)^{|m-n|/2}\beta^{|m-n|}e^{-\beta^2/4}L_{\min_{n,m}}^{(|m-n|)}(\beta^2/2)\delta_{(m+n) \bmod 2,0},$$

and when the offset flux is $\phi_{\text{off}} = \pi$ the matrix elements are

$$-E_J\langle\psi_m(\phi_k)|\sin(\hat{\phi}_k)|\psi_n(\phi_k)\rangle = -E_J\tfrac{1}{\sqrt{2^{n+m}n!m!}}2^{\min_{n,m}}(\min_{n,m})!(-1)^{(|m-n|-1)/2}\beta^{|m-n|}e^{-\beta^2/4}L_{\min_{n,m}}^{(|m-n|)}(\beta^2/2)\delta_{(m+n) \bmod 2,1},$$

where $L_a^{(b)}(x)$ is the generalized Laguerre polynomial. Diagonalizing $\hat{H}_k$ in the basis $\{\psi_n(\phi_k)\}_{n=0}^{D-1}$ for some fixed dimension D then gives approximations to the eigen-energies and eigenfunctions. In practice, for the regimes of interest, choosing $D \sim 80$ yields estimates of eigenenergies good to $\sim 10^{-6}$ in units of E_J.

III. MEASUREMENT OF NON-LOCAL ORDER PARAMETERS

A. Measurement of Wilson loops

Consider the measurement of the Wilson loop operator for the $U(1)$ QLM using spin-1 particles. We want a way to measure loop operators like

$$\hat{W}(\mathcal{C}) = \hat{S}^+ \otimes \hat{S}^- \otimes \cdots \otimes \hat{S}^+ \otimes \hat{S}^-,$$

on a spatial loop $\mathcal{C}$ on the lattice where

$$S^+ = \sqrt{2}\begin{pmatrix} 0 & 1 & 0 \\ 0 & 0 & 1 \\ 0 & 0 & 0 \end{pmatrix} = (S^-)^\dagger. \tag{24}$$

We will make use of the unitary Pauli $\hat{X}$ operator on qutrits:

$$\hat{X} = \begin{pmatrix} 0 & 1 & 0 \\ 0 & 0 & 1 \\ 1 & 0 & 0 \end{pmatrix} = \frac{\hat{S}^+}{\sqrt{2}} + \frac{(\hat{S}^-)^2}{2}.$$

The weighted expectation value of the unitary loop operator of length $|\mathcal{C}|$ (which is even on a square lattice) is

$$2^{|\mathcal{C}|/2}\langle\hat{X}\otimes\hat{X}^\dagger\otimes\cdots\otimes\hat{X}\otimes\hat{X}^\dagger\rangle = \langle(\hat{S}^+ + \tfrac{(\hat{S}^-)^2}{\sqrt{2}})\otimes(\hat{S}^- + \tfrac{(\hat{S}^+)^2}{\sqrt{2}})\otimes\cdots\otimes(\hat{S}^+ + \tfrac{(\hat{S}^-)^2}{\sqrt{2}})\otimes(\hat{S}^- + \tfrac{(\hat{S}^+)^2}{\sqrt{2}})\rangle.$$

If we restrict to the gauge invariant space of states then the expectation value takes the simple form

$$\langle\hat{V}(\mathcal{C})\rangle \equiv \langle\hat{X}\otimes\hat{X}^\dagger\otimes\cdots\otimes\hat{X}\otimes\hat{X}^\dagger\rangle = 2^{-|\mathcal{C}|/2}\langle\hat{W}(\mathcal{C})\rangle + 2^{-|\mathcal{C}|}\langle(\hat{W}^\dagger(\mathcal{C}))^2\rangle.$$

We can cancel the additional term using the modified unitary operator

$$\hat{X}(\phi) = \begin{pmatrix} 0 & 1 & 0 \\ 0 & 0 & 1 \\ e^{i\phi} & 0 & 0 \end{pmatrix} = \frac{\hat{S}^+}{\sqrt{2}} + e^{i\phi}\frac{(\hat{S}^-)^2}{2},$$

on one lattice spin (say the first spin) such that In the gauge invariant sector

$$\langle \hat{V}'(\mathcal{C})\rangle \equiv \langle \hat{X}(\pi)\otimes\hat{X}^\dagger(0)\otimes\cdots\otimes\hat{X}(0)\otimes\hat{X}^\dagger(0)\rangle = 2^{-|C|/2}\langle\hat{W}(\mathcal{C})\rangle - 2^{-|C|}\langle(\hat{W}^\dagger(\mathcal{C}))^2\rangle.$$

The sum of expectation values is $\langle\hat{V}(\mathcal{C})\rangle + \langle\hat{V}'(\mathcal{C})\rangle = 2^{-|C|/2}\langle\hat{W}(\mathcal{C})\rangle$.

Measurement of $\hat{V}(\mathcal{C})$ can be done by coupling the lattice of spin to a bosonic mode [43]. We first consider a realization of the measurement via a geometric phase gate using coherent state displacements of the mode, and second a realization using a single Fock state excitation.

In order to measure $\hat{V}(\mathcal{C})$ it is convenient to transform to a basis diagonal in the spin states:

$$\hat{V}(\mathcal{C}) = \hat{X}\otimes\hat{X}^\dagger\otimes\cdots\otimes\hat{X}\otimes\hat{X}^\dagger = \hat{W}^\dagger\hat{Z}^{\otimes|C|}\hat{W},$$

where

$$\hat{Z} = \begin{pmatrix} 1 & 0 & 0 \\ 0 & \xi & 0 \\ 0 & 0 & \xi^2 \end{pmatrix},$$

$\hat{W} = \hat{F}^\dagger\otimes\hat{F}\otimes\cdots\otimes\hat{F}^\dagger\otimes\hat{F}$, and the discrete Fourier transform is $\hat{F} = \frac{1}{\sqrt{3}}\sum_{r,s=0}^{2}\xi^{rs}|r\rangle\langle s|$ with $\xi = e^{i2\pi/3}$. Hence we can focus on generating evolution by the diagonal many body operator $\hat{Z}^{\otimes|C|}$.

1. *Geometric phase gate*

Let $\hat{a}$ and $\hat{a}^\dagger$ be creation and annihilation operators for a bosonic mode satisfying $[\hat{a},\hat{a}^\dagger] = 1$. The displacement operator acting on this mode is $\hat{D}(\alpha) = e^{\alpha\hat{a}^\dagger - \alpha^*\hat{a}}$, and the phase rotation operator is $\hat{R}(\theta) = e^{i\theta\hat{a}^\dagger\hat{a}}$. For any operator $\hat{O}$ acting on the lattice spins note the following identity

$$\hat{D}(\alpha e^{i\phi + i\theta\hat{O}}) = \hat{R}(\theta\hat{O})\hat{D}(\alpha e^{i\phi})\hat{R}(-\theta\hat{O}). \tag{25}$$

The following sequence produces a geometric phase gate on the spins which corresponds to evolution by an effective many-body Hamiltonian [43, 44]

$$\hat{U}(\phi,\theta,\Omega) = \hat{D}(-\beta)\hat{R}(\theta\hat{O})\hat{D}(-\alpha)\hat{R}(-\theta\hat{O})\hat{D}(\beta)\hat{R}(\theta\hat{O})\hat{D}(\alpha)\hat{R}(-\theta\hat{O}) = \exp(-i\Omega\sin(\theta\hat{O}+\phi)), \tag{26}$$

where $\phi = \arg(\alpha) - \arg(\beta)$ and $\Omega = |\alpha\beta|$. Note after this sequence, the bosonic mode is disentangled from the spins. In particular, if it begins in the vacuum then it ends in the vacuum state, and the first controlled phase rotation $\hat{R}(-\theta\hat{O})$ in Eq. (26) can be omitted. Choose $\hat{O}$ to be a sum over local operators on the spins along the loop $\mathcal{C}$: $\hat{O} = \sum_{j\in\mathcal{C}}\sum_{k=1}^{2} k|k\rangle_j\langle k|$, where $|0\rangle = |\hat{S}^z = 1\rangle, |1\rangle = |\hat{S}^z = 0\rangle, |2\rangle = |\hat{S}^z = -1\rangle$. The physical interaction required to generate the unitary $\hat{R}(\theta\hat{O})$ is dispersive coupling between the bosonic mode and the spins

$$\hat{H}_{\rm int} = -\chi\hat{a}^\dagger\hat{a}\sum_{j\in\mathcal{C}}\sum_{k=1}^{2} k|k\rangle_j\langle k|. \tag{27}$$

Specifically, $\hat{R}(\theta\hat{O}) = e^{-i\hat{H}_{\rm int}\tau}$ for $\tau = \theta/\chi$. It practice it may be simpler to implement in two steps with dispersive coupling to a single basis state $|0\rangle$ in each step: $\hat{R}(\theta\hat{O}) = F_1^\dagger e^{i\chi\tau_1\hat{a}^\dagger\hat{a}\sum_{j\in\mathcal{C}}|0\rangle_j\langle 0|}F_1F_2^\dagger e^{i\chi\tau_2\hat{a}^\dagger\hat{a}\sum_{j\in\mathcal{C}}|0\rangle_j\langle 0|}F_2$ with $\tau_2 = 2\tau_1 = \theta/\chi$ and the local state permutation unitaries $F_1 = |0\rangle\langle 1| + |1\rangle\langle 0| + |2\rangle\langle 2|$ and $F_2 = |0\rangle\langle 2| + |2\rangle\langle 0| + |1\rangle\langle 1|$.

There following parameter settings in the geometric phase gate is of interest:

$$\hat{U}(0,\frac{2\pi}{3},\frac{\pi}{\sqrt{3}}) = \frac{1}{3}\mathbf{1} + (\frac{1}{3} - \frac{1}{\sqrt{3}})\hat{Z}^{\otimes|C|} + (\frac{1}{3} + \frac{1}{\sqrt{3}})\hat{Z}^{\dagger\otimes|C|}.$$

Now we also need a coupling between an ancilla spin A and the bosonic field

$$\hat{H}^A_{\rm int} = -\chi\hat{a}^\dagger\hat{a}|1\rangle_A\langle 1|.$$

This will enable the gate $\hat{R}(\pi|1\rangle_A\langle 1|) = e^{-i\hat{H}^A_{\rm int}\tau}$ for $\tau = \pi/\chi$ which can be used to obtain a controlled displacement of the bosonic mode dependent on the state of the ancilla state:

$$\hat{D}(\beta|1\rangle_A\langle 1|) = \hat{D}(\beta/2)\hat{R}(\pi|1\rangle_A\langle 1|)\hat{D}(-\beta/2)R(-\pi|1\rangle_A\langle 1|) = |0\rangle_A\langle 0|\otimes\mathbf{1} + |1\rangle_A\langle 1|\otimes\hat{D}(\beta).$$

The following composition of the these primitive gates will enable a controlled many-body unitary conditioned on the state of the ancilla:

$$\hat{M}(\phi,\theta,\Omega) = \hat{D}(-\beta|1\rangle_A\langle 1|)\hat{R}(\theta\hat{O})\hat{D}(-\alpha)\hat{R}(-\theta\hat{O})\hat{D}(\beta|1\rangle_A\langle 1|)\hat{R}(\theta\hat{O})\hat{D}(\alpha)\hat{R}(-\theta\hat{O}) = |0\rangle_A\langle 0|\otimes\mathbf{1} + |1\rangle_A\langle 1|\otimes\hat{U}(\phi,\theta,\Omega). \tag{28}$$

Beginning with the ancilla in the state $|+_x\rangle_A = \frac{1}{\sqrt{2}}(|0\rangle + |1\rangle)$ and the lattice spins in the state $|\psi\rangle$, perform local rotations using W followed by the controlled many-body unitary, followed by the inverse local rotations:

$$\hat{W}^\dagger\hat{M}(\phi,\theta,\Omega)\hat{W}|\psi\rangle|+_x\rangle_A = \frac{1}{\sqrt{2}}(|\psi\rangle|0\rangle_A + \hat{W}\hat{U}(\phi,\theta,\Omega)\hat{W}^\dagger|\psi\rangle|1\rangle_A).$$

The measured polarization of the ancilla along the $\hat{x}$ and $\hat{y}$ directions is

$$\langle\hat{\sigma}^x_A\rangle(\phi,\theta,\Omega) = \Re[\langle\hat{W}\hat{U}(\phi,\theta,\Omega)\hat{W}^\dagger\rangle]$$
$$\langle\hat{\sigma}^y_A\rangle(\phi,\theta,\Omega) = \Im[\langle\hat{W}\hat{U}(\phi,\theta,\Omega)\hat{W}^\dagger\rangle],$$

where the expectation value on the right hand side is taken with respect to the spin lattice many-body state $|\psi\rangle$. For the aforementioned geometric phase gate parameters

$$\langle\hat{\sigma}^x_A\rangle(0,\tfrac{2\pi}{3},\tfrac{\pi}{\sqrt{3}}) = \tfrac{1}{3}(1+2\times\Re[\langle\hat{V}(\mathcal{C})\rangle])$$
$$\langle\hat{\sigma}^y_A\rangle(0,\tfrac{2\pi}{3},\tfrac{\pi}{\sqrt{3}}) = -\tfrac{2}{\sqrt{3}}\Im[\langle\hat{V}(\mathcal{C})\rangle].$$

Hence we can perform a non-demolition measurement of the real and imaginary parts of $V(\mathcal{C})$. In order to measure $V'(\mathcal{C})$, we use a very similar protocol but with the replacements: $\hat{W}\to\hat{W}' = \hat{F}'^\dagger\otimes\hat{F}\cdots\otimes\hat{F}'^\dagger\otimes\hat{F}$ where

$$\hat{F}' = \frac{1}{\sqrt{3}}\begin{pmatrix} 1 & \xi & \xi^2 \\ -1 & -\xi^2 & -\xi \\ 1 & 1 & 1 \end{pmatrix},$$

acts on every other (say even labelled) spins, and choose the interaction between the spin and the bosonic mode to have the opposite sign, $\chi\to-\chi$, for the even labelled spins, which is equivalent to changing $\theta\to-\theta$ for the unitary evolution on those spins. This enables a non-demolition measurement of the Wilson loop.

2. *Single photon mediated gate*

If single Fock states of the bosonic mode can be prepared then the measurement protocol is significantly simplified. Consider a single Fock state of a photonic mode which is a superposition of polarization modes: $|\phi\rangle_{\text{field}} = \frac{1}{\sqrt{2}}(\hat{a}^\dagger_+ + \hat{a}^\dagger_-)|vac\rangle = \frac{1}{\sqrt{2}}(|1\rangle_+ + |1\rangle_-)$. Also let the lattice spins interact with the photon via a polarization dependent coupling

$$\hat{H}_{\text{int}} = -\chi\hat{a}^\dagger_-\hat{a}_-\sum_{j\in\mathcal{C}}\sum_{k=1}^{2}k|k\rangle_j\langle k|.$$

Then the conjugated evolution for a time $\tau = 2\pi/3\chi$ from the initial state is

$$\hat{W}^\dagger e^{-i\hat{H}_{\text{int}}\tau}\hat{W}|\psi\rangle|\phi\rangle_{\text{field}} = \frac{1}{\sqrt{2}}(|\psi\rangle|1\rangle_+\hat{V}(\mathcal{C})|\psi\rangle|1\rangle_-)$$

The measured polarization of the field mode in the bases $|\pm_x\rangle = (|1\rangle_+ \pm |1\rangle_-)/\sqrt{2}$ and $|\pm_y\rangle = (|1\rangle_+ \pm i|1\rangle_-)/\sqrt{2}$ is

$$\langle\hat{\sigma}^x_{\text{field}}\rangle = \Re[\langle\hat{V}(\mathcal{C})\rangle]$$
$$\langle\hat{\sigma}^y_{\text{field}}\rangle = \Im[\langle\hat{V}(\mathcal{C})\rangle].$$

A similar measurement of $V'(\mathcal{C})$ can be made with the same adaptations as in the geometric phase gate implementation.

While conceptually simpler, this method is in practice more challenging than the geometric phase gate because quantum control at the single photon level is needed, while in the former, only Gaussian states and operations on the bosonic mode are required.

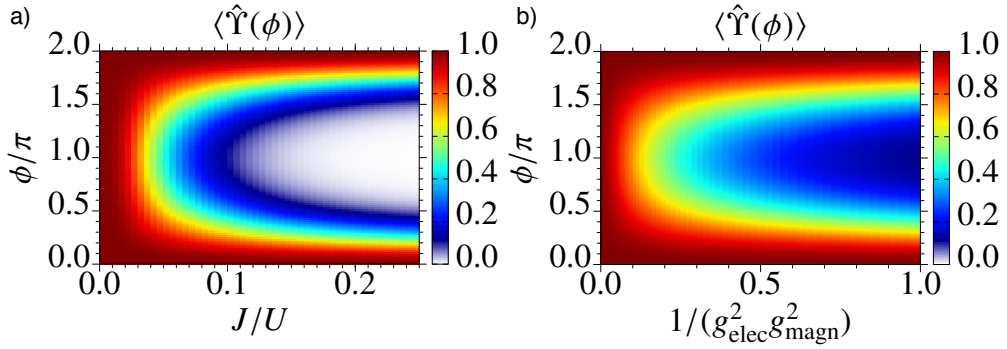

FIG. 5. Expectation value of the 't Hooft disorder parameter $\hat{\Upsilon}(\phi)$ for the ladder geometry in Fig. 3 of main text. a) Value in the ground state of the two body Hamiltonian $\hat{H}_{\rm imp}$ with $V = 0$. b) Value in the ground state of the pure gauge model $\hat{H}_{\rm QLM}$. Qualitatively this shows that the implementation Hamiltonian is well described by the effective pure gauge model for $J/U \ll 1$

B. Measurement of 't Hooft disorder operator

The 't Hooft disorder operator acting on n spins-1 particles for $U(1)$ QLM model is

$$\hat{\Upsilon}(\delta) = e^{-i\delta\hat{S}^z_0} \otimes e^{i\delta\hat{S}^z_1} \otimes \cdots \otimes e^{-i\delta\hat{S}^z_{n-2}} \otimes e^{i\delta\hat{S}^z_{n-1}}.$$

where it is assumed the spins are ordered on a line in the dual lattice.

1. *Geometric phase gate*

The protocol is quite is quite similar to that for the Wilson loop measurement. Choose the spin operator to be $\hat{O} = \sum_{j=0}^{n-1}(|\hat{S}^z = 1\rangle_j\langle\hat{S}^z = 1| - |\hat{S}^z = -1\rangle_j\langle\hat{S}^z = -1|)$. Now follow the same steps as in Eq. (28) but where $\theta \to -\theta$ for the even labelled spins, which can be obtained by picking $\chi \to -\chi$ in the interaction $H_{\rm int}$.

The measurement is easiest for the operator $\hat{\phi}(\delta = \pi)$. In that case, we can pick $\hat{O} = \sum_{j=0}^{n-1}|\hat{S}^z = 0\rangle_j\langle\hat{S}^z = 0|$ and use the angle $\theta = \pi$ which means when needed one should evolve via the interaction $H_{\rm int}$ for a time $\tau = \pi/|\chi|$. The unitary $U(\frac{\pi}{2}, \pi, \frac{\pi}{2}) = (-i)^n\hat{\phi}(\pi)$, and performing the controlled unitary operator on the initial state

$$\hat{M}(\frac{\pi}{2}, \pi, \frac{\pi}{2})|\psi\rangle|+_x\rangle_A = \frac{1}{\sqrt{2}}(|\psi\rangle|0\rangle_A + (-i)^n\hat{\phi}(\pi)|\psi\rangle|1\rangle_A).$$

The measured polarization of the ancilla along the $\hat{x}$ and $\hat{y}$ directions is

$$\langle\hat{\sigma}^x_A\rangle(\tfrac{\pi}{2}, \pi, \tfrac{\pi}{2}) = \Re[\langle(-i)^n\hat{\phi}(\pi)\rangle]$$
$$\langle\hat{\sigma}^y_A\rangle(\tfrac{\pi}{2}, \pi, \tfrac{\pi}{2}) = \Im[\langle(-i)^n\hat{\phi}(\pi)\rangle],$$

Hence we can perform a non-demolition measurement of the 't Hooft string $\hat{\Upsilon}(\pi)$.

2. *Single photon mediated gate*

The single photon mediated gate easily enables measurement of $\hat{\Upsilon}(\delta)$ for any δ. Use the polarization dependent coupling which alternates sign on every other spin,

$$\hat{H}_{\rm int} = -\chi\hat{a}^\dagger_-\hat{a}_- \sum_{j=0}^{n-1}(-1)^j(|\hat{S}^z = 1\rangle_j\langle\hat{S}^z = 1| - |\hat{S}^z = -1\rangle_j\langle\hat{S}^z = -1|).$$

Then, following in the same manner as in the previous section where we measure the Wilson loop operator with a single photon mediated gate, the evolution from the initial state for a time $\tau = \delta/|\chi|$ is

$$e^{-i\hat{H}_{\rm int}\tau}|\psi\rangle|\phi\rangle_{\rm field} = \frac{1}{\sqrt{2}}(|\psi\rangle|1\rangle_+ + \hat{\phi}(\delta)|\psi\rangle|1\rangle_-)$$

The measured polarization of the field mode is

$$\langle\hat{\sigma}^x_{\rm field}\rangle = \Re[\langle\hat{\phi}(\delta)\rangle]$$
$$\langle\hat{\sigma}^y_{\rm field}\rangle = \Im[\langle\hat{\phi}(\delta)\rangle].$$

C. Fidelity of the measurement

1. *Effects due to cavity decay and spin depolarization*

The process fidelity for many-spin gates generated via coupling to bosonic channels was calculated in Ref. [44]. For the uncontrolled geometric phase gate $U(\phi,\theta,\Omega)$ acting on qubits, it was shown that when the only form of decoherence is field decay at a rate κ, the process fidelity is lower bounded by $F = 1-\frac{\pi\Omega\kappa}{|\chi|}(e^{-3\theta\kappa/2|\chi|}+e^{-\theta\kappa/2|\chi|})(1+\frac{\pi\kappa}{2|\chi|})$, where χ is the spin-field dispersive coupling. Including also collective depolarization of the spins at a rate γ over a time period t for the total gate, giving rise to an error probability $p = 1-e^{-\gamma t}$, as well as independent depolarization at a rate γ_i acting on each of the n spins involved, giving rise independent depolarization error rate $p_i = 1-e^{-\gamma_i\tau}$, the process fidelity is $F_{\rm pro} > (1-np_i-p)F$.

We can obtain a fidelity bound $F^{(gp)}_{\rm pro}(\theta,\Omega)$ for the geometric phase realization of controlled unitary operator $\hat{M}(\phi,\theta,\Omega)$ by a simple adaptation of the above calculation. Coherent state displacements can be made very quickly with respect to other time scales in the system and the number of interaction gates in $\hat{M}(\phi,\theta,\Omega)$ is 7, i.e., 4 more than those needed for $U(\phi,\theta,\Omega)$ (assuming the initial state of the bosonic mode is vacuum). Depolarization of the ancilla spin acts like collective decoherence in the system and we can assume it occurs at the same rate as independent error (i.e., $p = p_i = 1-e^{-\gamma t}$). For dispersive coupling the total time for the gate $\hat{M}$ is $t \approx (4\pi+6\theta)/|\chi|$, where we have assumed that the maximum dispersive coupling to any basis state of the spins is χ so that each controlled rotation $R(\theta\hat{O})$ actually takes time $2\theta/|\chi|$. The entire process fidelity for measuring the many body operator, including implementing the controlled unitary $\hat{M}(\phi,\theta,\Omega)$ using the geometric phase gate on n spins (including 1 ancilla spin), followed by measurement of the ancilla is then

$$F^{(gp)}_{\rm pro}(\theta,\Omega) > \eta_A\Big(1-n(1-e^{-(4\pi+6\theta)\gamma/|\chi|})\Big)\Big(1-\tfrac{\pi\Omega\kappa}{|\chi|}(e^{-3\theta\kappa/|\chi|}+e^{-\theta\kappa/|\chi|})(1+\tfrac{\pi\kappa}{2|\chi|})\Big). \quad (29)$$

where $\eta_A \leq 1$ describes finite detection fidelity of the ancilla spin.

For the Wilson loop measurement $\Omega = \pi/\sqrt{3}, \theta = 2\pi/3$, while for the 't Hooft string $\hat{\Upsilon}(\pi)$ measurement $\Omega = \pi/2, \theta = \pi/2$. The reason why we take $\theta = \pi/2$ for the latter is that in Eq. (29) we assumed that twice the field-spin interaction time was needed to accumulate the phase on one of the basis states while, as described in the section where we measure the 't Hooft disorder string operator with a single photon mediated gate, for measuring $\hat{\Upsilon}(\pi)$ only one basis state need interact with the field mode.

For a realization of the controlled unitary by a single photon gate the fidelity is enhanced significantly using feed forward control [44]. During the gate the cavity trapping the field mode can be monitored for leakage by detectors. A case of null detection improves the performance of the gate relative to an unmonitored cavity, and if a detection is seen then the gate can be repeated. The total process fidelity for measuring the many body operator is

$$F^{(sp)}_{\rm pro}(\theta) > \eta_p\Big(1-n(1-e^{-\gamma\bar{t}(\theta)})\Big). \quad (30)$$

where $\eta_p \leq 1$ describes finite single photon detection fidelity, and where the mean gate time is

$$\bar{t}(\theta) = \frac{(1+e^{2\theta\kappa/|\chi|})(2\theta)^2\kappa/|\chi|^2}{2\theta\kappa/|\chi|+e^{2\theta\kappa/|\chi|}-1}. \quad (31)$$

Here, for the Wilson loop measurement $\theta = 2\pi/3$, while for measurement of the 't Hooft string $\hat{\Upsilon}(\phi)$, $\theta = \phi/2$.

2. *Effects of inhomogeneity*

Here we consider the effects of inhomogeneous coupling of spins to the cavity. This can be modeled by modifying the dispersive interaction as

$$\hat{H}_{\rm int} = -\hat{a}^\dagger\hat{a}\sum_{j\in C}\chi_j\sum_{k=1}^{2}k|k\rangle_j\langle k|, \quad (32)$$

where the dispersive coupling strength χ may vary in space. To simplify the analysis, let's consider a system of $|C| = n$ qubits and a target many body gate $U_{\rm target} = e^{-i\Omega Z^{\otimes n}}$ (without loss of generality pick $= n \bmod 4 = 1$). According to Eq. 26, the

general form for the unitary operator generated using the geometric phase gate is $U(\phi,\theta,\Omega) = \exp(-i\Omega\sin(\theta\hat{O}+\phi))$ and we get our target unitary by picking $\phi = 0$, $\theta = \frac{\pi}{2}$, and $\hat{O} = \sum_j \hat{Z}_j$ where $\hat{Z} = |0\rangle\langle 0| - |1\rangle\langle 1|$. This could be generated by a uniform dispersive coupling: $\hat{H}_{\rm int} = -\hat{a}^\dagger\hat{a}\sum_j \chi_j\hat{Z}_j$ with $\chi_j = \chi\forall j$. In the presence of inhomogeneities, the actual unitary will be $U = \exp(-i\Omega\sin(\sum_j(\frac{\pi}{2}(1+\varepsilon_j)\hat{Z}_j))$ where $\varepsilon_j = (\chi_j-\chi)/\chi$. We can write this as

$$U(0,\tfrac{\pi}{2},\Omega) \;=\; \exp(-i\tfrac{\Omega}{2i}((iZ)^{\otimes n}\prod_j(\cos(\tfrac{\pi\varepsilon_j}{2}) + i\sin\tfrac{\pi\varepsilon_j}{2}\hat{Z}_j) - (-iZ)^{\otimes n}\prod_j(\cos\tfrac{\pi\varepsilon_j}{2} - i\sin\tfrac{\pi\varepsilon_j}{2}\hat{Z}_j).$$

If the value of the inhomogeneity is known, say by gate tomography, then we can adjust $\Omega \to \Omega/\prod_j\cos\frac{\pi\varepsilon_j}{2} = \tilde{\Omega}$ by simply adjusting the magnitude of displacement operators during the geometric phase gate. Now

$$\begin{aligned} U(0,\tfrac{\pi}{2},\tilde{\Omega}) &= \exp(-i\tfrac{\Omega}{2i}((iZ)^{\otimes n}\prod_j(1+i\tan\tfrac{\pi\varepsilon_j}{2}\hat{Z}_j) - (-iZ)^{\otimes n}\prod_j(1-i\tan\tfrac{\pi\varepsilon_j}{2}\hat{Z}_j) \\ &= U_{\rm target}\times\exp(i\Omega\textstyle\sum_{a\neq b}\tan\frac{\pi\varepsilon_a}{2}\tan\frac{\pi\varepsilon_b}{2}\prod_{r\neq a,b}\hat{Z}_r) \\ &\quad\times\exp(-i\Omega\textstyle\sum_{a\neq b\neq c\neq d}\tan\frac{\pi\varepsilon_a}{2}\tan\frac{\pi\varepsilon_b}{2}\tan\frac{\pi\varepsilon_c}{2}\tan\frac{\pi\varepsilon_d}{2}\prod_{r\neq a,b,c,d}\hat{Z}_r)\times\cdots. \end{aligned}$$

The error $\mathcal{E}$ in the gate implementation due to inhomogeneities can be quantified as follows

$$\mathcal{E} \equiv ||U_{\rm target}^{-1}U(0,\frac{\pi}{2},\tilde{\Omega}) - \mathbf{1}||_2 = ||\mathbf{1} - [e^{i\Omega\sum_{a\neq b}\tan\frac{\pi\varepsilon_a}{2}\tan\frac{\pi\varepsilon_b}{2}\prod_{r\neq a,b}\hat{Z}_r}][e^{-i\Omega\sum_{a\neq b\neq c\neq d}\tan\frac{\pi\varepsilon_a}{2}\tan\frac{\pi\varepsilon_b}{2}\tan\frac{\pi\varepsilon_c}{2}\tan\frac{\pi\varepsilon_d}{2}\prod_{r\neq a,b,c,d}\hat{Z}_r}]\cdots||_2,$$

where the operator norm on an operator A is $||A||_2 = \sup_x\frac{||Ax||_2}{||x||_2}$. Define $\varepsilon = \max_j\varepsilon_a$, then

$$\begin{aligned} \mathcal{E} &\leq ||-i\textstyle\sum_{j=1}^{\lfloor n\rfloor/2}(-1)^j\tan^{2j}\frac{\pi\varepsilon}{2}\sum_{\{a_1,\ldots a_{2j}\}}\prod\hat{Z}_{a_k}||_2 \\ &\leq \textstyle\sum_{j=1}^{\lfloor n\rfloor/2}\tan^{2j}\frac{\pi\varepsilon}{2}\sum_{\{a_1,\ldots a_{2j}\}}||\prod\hat{Z}_{a_k}||_2 \\ &= \textstyle\sum_{j=1}^{\lfloor n\rfloor/2}\binom{n}{2j}\tan^{2j}\frac{\pi\varepsilon}{2} \\ &= \tfrac{1}{2}((\tan\tfrac{\pi\varepsilon}{2}-1)^n + (\tan\tfrac{\pi\varepsilon}{2}+1)^n - 2). \end{aligned}$$

where the sum over member of the set $\{a_1,\ldots a_{2j}\}$ is over the choices of $2j$ distinct spin locations. For $\varepsilon \ll 1$ the error is, $||U_{\rm target}^{-1}U(0,\frac{\pi}{2},\tilde{\Omega}) - \mathbf{1}||_2 \approx n(n-1)(\frac{\pi}{2})^2\varepsilon^2/2$. For gates with different rotation angles θ, the error will be roughly the same with the replacement $(\frac{\pi}{2})^2 \to \theta^2$. The many body gates used for measurement of loop and strings in the spin-1 realization of quantum link models can be obtained by compositions of many body gates on qubit subspaces as described above.